NATIONAL ADVISORY COMMITTEE FOR AERONAUTICS

REPORT No. 604

PRESSURE-DISTRIBUTION MEASUREMENTS AT LARGE ANGLES OF PITCH ON FINS OF DIFFERENT SPAN-CHORD RATIO ON A 1/40-SCALE MODEL OF THE U. S. AIRSHIP "AKRON"

By JAMES G. McHUGH

1937

For sale by the Superintendent of Documents, Washington, D. C. - - - - Price 10 cents
Subscription price, $3 per year

AERONAUTIC SYMBOLS

1. FUNDAMENTAL AND DERIVED UNITS

	Symbol	Metric		English	
		Unit	Abbreviation	Unit	Abbreviation
Length	l	meter	m	foot (or mile)	ft. (or mi.)
Time	t	second	s	second (or hour)	sec. (or hr.)
Force	F	weight of 1 kilogram	kg	weight of 1 pound	lb.
Power	P	horsepower (metric)		horsepower	hp.
Speed	V	kilometers per hour	k.p.h.	miles per hour	m.p.h.
		meters per second	m.p.s.	feet per second	f.p.s.

2. GENERAL SYMBOLS

W, Weight$=mg$

g, Standard acceleration of gravity$=9.80665$ m/s^2 or 32.1740 ft./sec.^{2}

m, Mass$=\frac{W}{g}$

I, Moment of inertia$=mk^2$. (Indicate axis of radius of gyration k by proper subscript.)

μ, Coefficient of viscosity

ν, Kinematic viscosity

ρ, Density (mass per unit volume)

Standard density of dry air, 0.12497 kg-m^{-4}-s^2 at 15° C. and 760 mm; or 0.002378 lb.-ft.$^{-4}$ sec.^{2}

Specific weight of "standard" air, 1.2255 kg/m^3 or 0.07651 lb./cu. ft.

3. AERODYNAMIC SYMBOLS

S, Area

S_w, Area of wing

G, Gap

b, Span

c, Chord

$\frac{b^2}{S}$, Aspect ratio

V, True air speed

q, Dynamic pressure$=\frac{1}{2}\rho V^2$

L, Lift, absolute coefficient $C_L=\frac{L}{qS}$

D, Drag, absolute coefficient $C_D=\frac{D}{qS}$

D_0, Profile drag, absolute coefficient $C_{D_0}=\frac{D_0}{qS}$

D_i, Induced drag, absolute coefficient $C_{D_i}=\frac{D_i}{qS}$

D_p, Parasite drag, absolute coefficient $C_{D_p}=\frac{D_p}{qS}$

C, Cross-wind force, absolute coefficient $C_C=\frac{C}{qS}$

R, Resultant force

i_w, Angle of setting of wings (relative to thrust line)

i_t, Angle of stabilizer setting (relative to thrust line)

Q, Resultant moment

Ω, Resultant angular velocity

$\rho\frac{Vl}{\mu}$, Reynolds Number, where l is a linear dimension (e.g., for a model airfoil 3 in. chord, 100 m.p.h. normal pressure at 15° C., the corresponding number is 234,000; or for a model of 10 cm chord, 40 m.p.s., the corresponding number is 274,000)

C_p, Center-of-pressure coefficient (ratio of distance of c.p. from leading edge to chord length)

α, Angle of attack

ϵ, Angle of downwash

α_0, Angle of attack, infinite aspect ratio

α_i, Angle of attack, induced

α_a, Angle of attack, absolute (measured from zero-lift position)

γ, Flight-path angle

REPORT No. 604

PRESSURE-DISTRIBUTION MEASUREMENTS AT LARGE ANGLES OF PITCH ON FINS OF DIFFERENT SPAN-CHORD RATIO ON A 1/40-SCALE MODEL OF THE U. S. AIRSHIP "AKRON"

By JAMES G. McHUGH

Langley Memorial Aeronautical Laboratory

153730—37——1

NATIONAL ADVISORY COMMITTEE FOR AERONAUTICS

HEADQUARTERS, NAVY BUILDING, WASHINGTON, D. C.

LABORATORIES, LANGLEY FIELD, VA.

Created by act of Congress approved March 3, 1915, for the supervision and direction of the scientific study of the problems of flight (U. S. Code, Title 50, Sec. 151). Its membership was increased to 15 by act approved March 2, 1929. The members are appointed by the President, and serve as such without compensation.

TECHNICAL COMMITTEES

AERODYNAMICS
POWER PLANTS FOR AIRCRAFT
AIRCRAFT MATERIALS
AIRCRAFT STRUCTURES
AIRCRAFT ACCIDENTS
INVENTIONS AND DESIGNS

Coordination of Research Needs of Military and Civil Aviation

Preparation of Research Programs

Allocation of Problems

Prevention of Duplication

Consideration of Inventions

LANGLEY MEMORIAL AERONAUTICAL LABORATORY

LANGLEY FIELD, VA.

Unified conduct, for all agencies, of scientific research on the fundamental problems of flight.

OFFICE OF AERONAUTICAL INTELLIGENCE

WASHINGTON, D. C.

Collection, classification, compilation, and dissemination of scientific and technical information on aeronautics.

REPORT No. 604

PRESSURE-DISTRIBUTION MEASUREMENTS AT LARGE ANGLES OF PITCH ON FINS OF DIFFERENT SPAN-CHORD RATIO ON A 1/40-SCALE MODEL OF THE U. S. AIRSHIP "AKRON"

By James G. McHugh

SUMMARY

Pressure-distribution measurements on a 1/40-scale model of the U. S. airship "Akron" were conducted in the N. A. C. A. 20-foot wind tunnel.

The measurements were made on the starboard fin of each of four sets of horizontal tail surfaces, all of approximately the same area but differing in span-chord ratio, for five angles of pitch varying from 11.6° to 34°, for four elevator angles, and at air speeds ranging from 56 to 77 miles per hour. Pressures were also measured at 13 stations along the rear half of the port side of the hull at one elevator setting for the same five angles of pitch and at an air speed of approximately 91 miles per hour.

The maximum pressures recorded on the leading edge of the fins, for pitch angles up to 20°, were approximately the same for all fins tested regardless of span-chord ratio. At angles of pitch above 20° the maximum fin pressures increased with decreasing span-chord ratio. A negative pressure of 13 times the dynamic pressure of the undisturbed air stream was measured on the fin of lowest span-chord ratio at a pitch angle of 34°. The pitching moment contributed by the after portion of the hull increased with pitch until, at the maximum angles tested, it was approximately equal to the moment contributed by the fins. The normal force on the fin and the moment of forces about the fin root were determined. The results indicate that, ignoring the effect on drag, it would be advantageous from structural considerations to use a fin of lower span-chord ratio than that used on the "Akron."

INTRODUCTION

The task of obtaining load measurements on a full-scale airship in free flight is difficult and, consequently, only a small amount of reliable flight data on airship loads is available. Many wind-tunnel tests of scale models have been made but, since the scale of an airship model for wind-tunnel tests must of necessity be very small, the results obtained are in some cases of questionable value.

The results of previous pressure-distribution measurements on the hull and fins of a relatively large (1/40-scale) model of the U. S. airship *Akron* fitted with fins of the type used on the full-scale airship and tested at angles of pitch from 0° to 18° are presented in reference 1. Although such a range of angles of pitch would not be exceeded under normal operating conditions, it appears possible that much larger angles of pitch might be encountered in severe gusts. No information concerning the magnitude of fin loads and pressures encountered at larger pitch angles has been available, but the results of reference 1 indicated that a high concentration of load near the tip would be obtained.

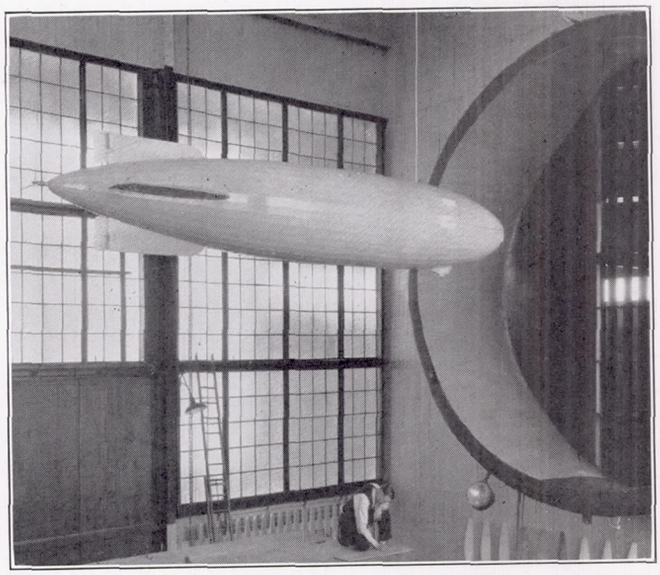

FIGURE 1.—The 1/40-scale model of the *Akron* mounted in the 20-foot wind tunnel.

At the request of the Bureau of Aeronautics, Navy Department, the investigation herein reported was made to obtain information concerning loads at high angles of pitch and to determine good fin proportions. The 1/40-scale airship model used in the investigation reported in reference 1 was tested through a range of pitch angles from 12° to 34° with the object of determining: (1) The effect of span-chord ratio on the aerodynamic forces acting on the fins of airships; (2) the effect of slots between the fin and the hull on pressure distribution over the fin; and (3) the effect of changes

in fin span-chord ratio on pressure distribution over the hull.

It is believed that the relatively large scale of the model here used, the high pitch angles included, and the fact that simultaneous measurements of pressure were made on both surfaces of an entire fin greatly enhance the value of these results.

APPARATUS AND TESTS

The airship model used in these tests is described in detail in reference 1. The method of mounting it in the wind tunnel is shown in figure 1 and is essentially as described in reference 2, with the exception that for these tests the model was suspended 3½ feet above the center line of the tunnel. The tests were made in the N. A. C. A. 20-foot wind tunnel (reference 3).

In order to determine the effect of different fins on the pressure distribution over the rear part of the hull, 162 pressure orifices distributed among 13 stations on the port side of the model were used. The location of the stations and the distribution of the orifices around the hull are shown in figure 2. Principal dimensions of the hull and fins are given in table I.

The fins were of laminated wood. Pressure orifices were installed by splitting the fins at their plane of symmetry, drilling small holes at the point where pressures were to be measured, inserting short lengths of 1/32-inch (inside diameter) copper tubing therein until they protruded a minute distance beyond the outer surface of the fin, and then, after alining the free ends of the copper tubes in such manner that they protruded through the inboard edge, gluing the two halves of the fin together. The ends of the copper tubing projecting through the fin surfaces were ground flush, thereby forming a smooth pressure orifice.

Four sets of horizontal tail surfaces, designated Mark II fin, fin 3, fin 3–A, and fin 4 (figs. 3 to 7), all of approximately the same area but of different span-chord ratios, were tested. The Mark II fin was the type used on the *Akron*. Fins 3 and 4 were basically similar but their span-chord ratios were changed by cutting areas off the inboard edge and adding an equivalent area at the forward part of the fin in such manner that the position of the elevator axis, the edge shape, and the radius of the tip plan form remained constant for all fins. Fin 3–A was similar to fin 3 except for a change in the plan form of the forward part of the fin. An additional type of fin was obtained by altering the Mark II fin so as to form a slot between the inboard edge of the fin and the hull of the ship. Two slot widths (⅜ inch and ¾ inch) were used. The longitudinal location of the slot on the fin, which corresponded to a location between frame 0 and frame 17. 5 of the full-scale airship, is shown by dotted lines in figure 3. Figure 8 shows the fin with slot mounted for tests.

Pressure orifices were installed in pairs on fins Mark II, 3, and 4. One orifice of each pair opened on the upper surface and the other, on the lower surface of the fin. In the case of fin 3–A, pressure orifices were installed only on the upper surface. On all the

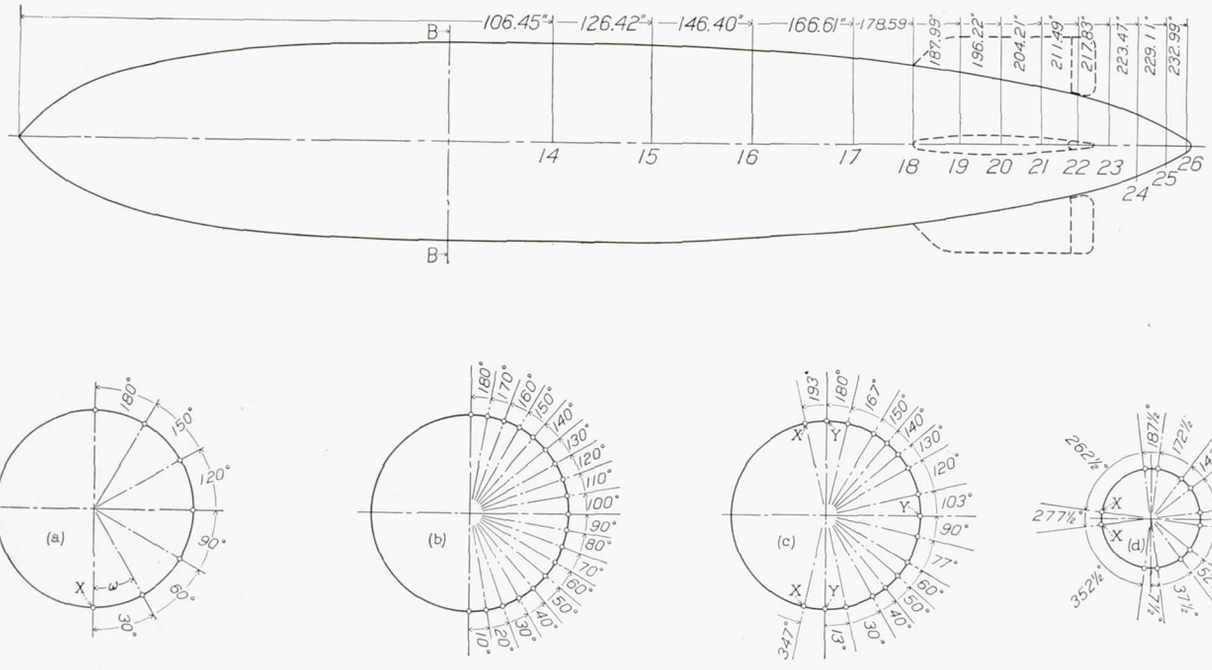

(a) Typical sections in direction B–B at stations 14 and 16 showing radial locations of orifices in hull. Orifice marked X at station 16 only.

(b) Typical sections in direction B–B at stations 15 and 17 showing radial locations of orifices in hull.

(c) Typical sections in direction B–B at stations 18, 19, 20, and 21 showing radial locations of orifices in hull. Two orifices marked X at stations 18, 20, and 21 only. Three orifices marked Y at station 18 only.

(d) Typical sections in direction B–B at stations 22, 23, 24, 25, and 26 showing radial locations of orifices in hull. Two orifices marked X at stations 22 and 23 only.

FIGURE 2.—Locations of orifices for the pressure measurement on a 1/40-scale model of the *Akron*. All dimensions given in inches.

fins the pressure orifices were located to facilitate fairing of the pressure diagram; the locations are shown in figures 3 to 6.

Two multiple-tube photographic recording manometers, each composed of a circular bank of 100 glass tubes, were mounted on pivots inside the model and were free to swing about a horizontal axis at right angles to the longitudinal axis of the ship, thus allowing the manometers to remain level for any angle of pitch. The manometers were electrically operated by remote control from the test chamber floor. Photostat paper was automatically drawn around the outer circumference of the bank of tubes, and exposure was made by flashing a lamp at the center of the bank of tubes.

Two simultaneous records, one for each manometer, gave for one pitch angle a complete diagram of the pressure distribution over both surfaces of a fin. Two sets of pressure measurements were made at each pitch angle and an average of the two records was used in plotting the pressure diagram. In order to provide a reference line on the pressure records, six of the glass tubes spaced equidistantly around the manometer were connected to the reference pressure, which for these tests was the static pressure in the test chamber.

With the exception of the Mark II fin, which was tested with and without elevator counterbalances, all fins were tested without counterbalances. In all cases the control car was installed on the hull of the model. All pressure-distribution measurements were made on the starboard fin and for all fins tested the vertical fins were of the Mark II type with rudder neutral and the airship at 0° yaw.

The tests herein reported are listed in the following table:

PRESSURE MEASUREMENTS ON HULL

Fin	Elevator angle (deg.)	Nominal pitch angle (deg.)	Approximate velocity (m. p. h.)
Mark II	20	12, 18, 24, 30, 36	91
3	20	12, 18, 24, 30, 36	91
4	20	12, 18, 24, 30, 36	91

PRESSURE MEASUREMENTS ON FINS

[No pressure-distribution measurements were taken on the elevators]

Fin	Elevator angle (deg.)	Nominal pitch angle (deg.)	Approximate velocity (m. p. h.)
Mark II [1]	0, 10, 20	12, 18, 24, 30, 36	69
Mark II	20	18, 30	77
Mark II, ⅜-inch slot	20	12, 18, 24, 30	77
Mark II, ¾-inch slot	20	12, 18, 24, 30	77
3	−15, 0, 10, 20	12, 18, 24, 30, 36	74
3-A	−15, 0, 10, 20	12, 18, 24, 30, 36	56
4	−15, 0, 10, 20	12, 18, 24, 30, 36	56

[1] With counterbalances.

ACCURACY

The sources of error that affect the pressure-distribution measurements are:

(1) Errors in measurements of the manometer deflection.

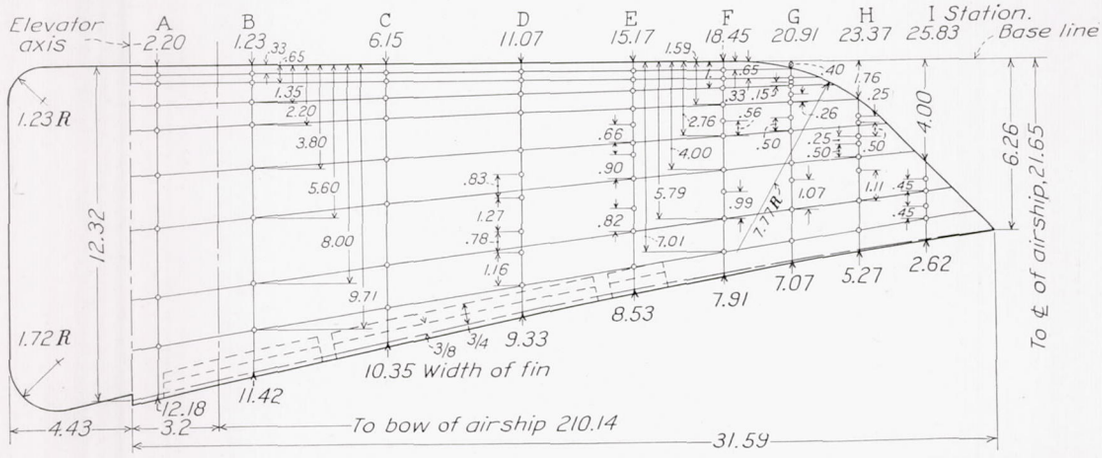

FIGURE 3.—Dimensions and orifice locations. Mark II fin; 1/40-scale model of the *Akron;* slot locations are shown in dotted lines; all dimensions given in inches.

(2) Oscillation of the manometers.

(3) Fluctuation in velocity and direction of the air stream.

(4) Shrinkage of the photostat paper.

The error due to (1) is considered to be small. The errors due to (1), (2), and (3) are of the order of ±2 percent for low pitch angles. At high pitch angles the error is considerably greater, as shown by comparison of check tests. The errors from (4) were found, in general, to be less than 1 percent for all cases.

RESULTS

The great amount of data derived from these tests makes it impractical to present them in their entirety. Consequently, only the portion required for the final analysis of the results is presented.

Final results of the pressure measurements are presented in terms of dynamic pressure q of the air stream. All pressures are referred to the test-chamber pressure, and no correction has been made for the difference between the static pressure in the air stream and the reference pressure. Application of this correction would have no effect on the integrated values of normal force on the fins. Pressures were measured on both the upper and lower surfaces of the fins (except for fin

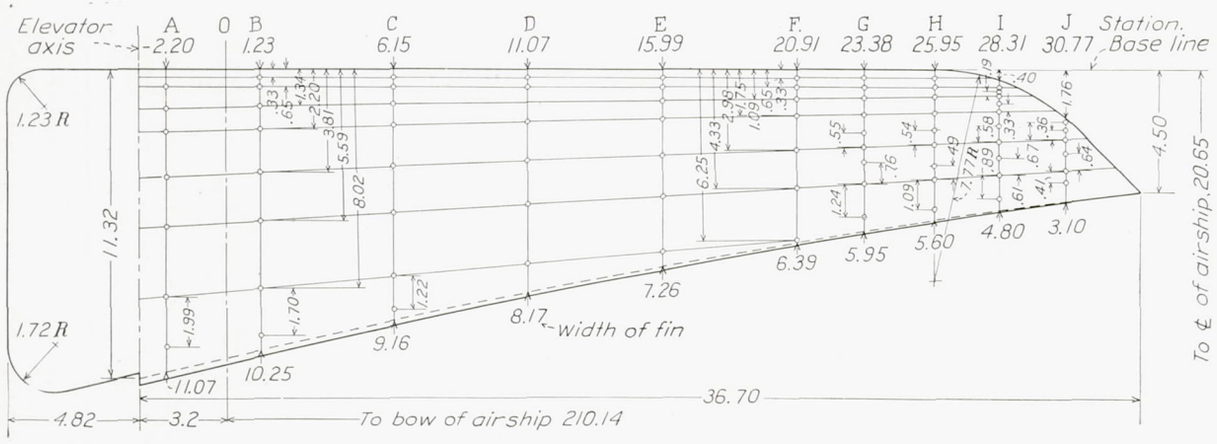

FIGURE 4.—Dimensions and orifice locations. Fin 3; 1/40-scale model of the *Akron;* all dimensions given in inches.

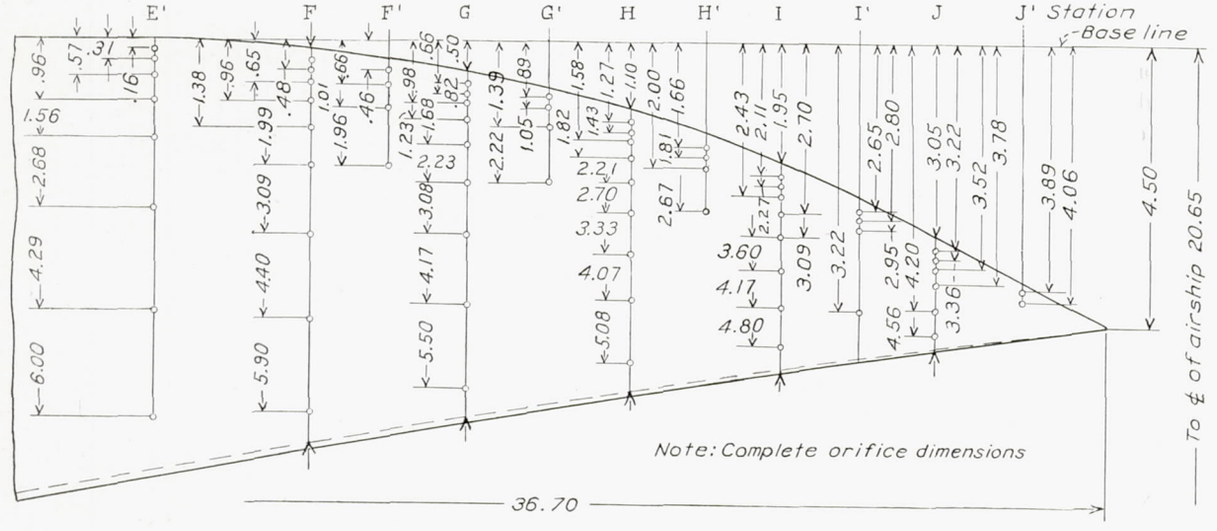

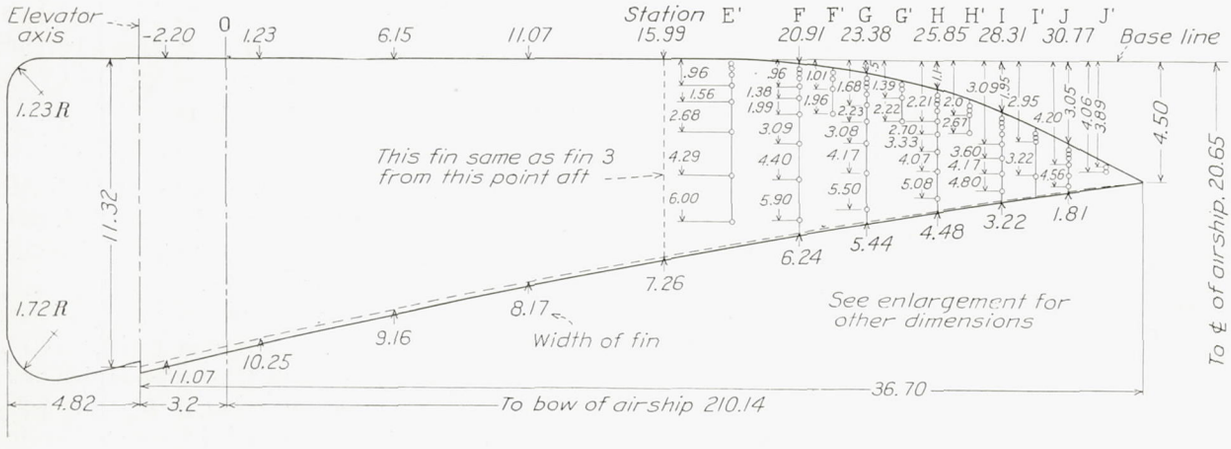

FIGURE 5.—Dimensions and orifice locations. Fin 3-A; 1/40-scale model of the *Akron;* all dimensions given in inches.

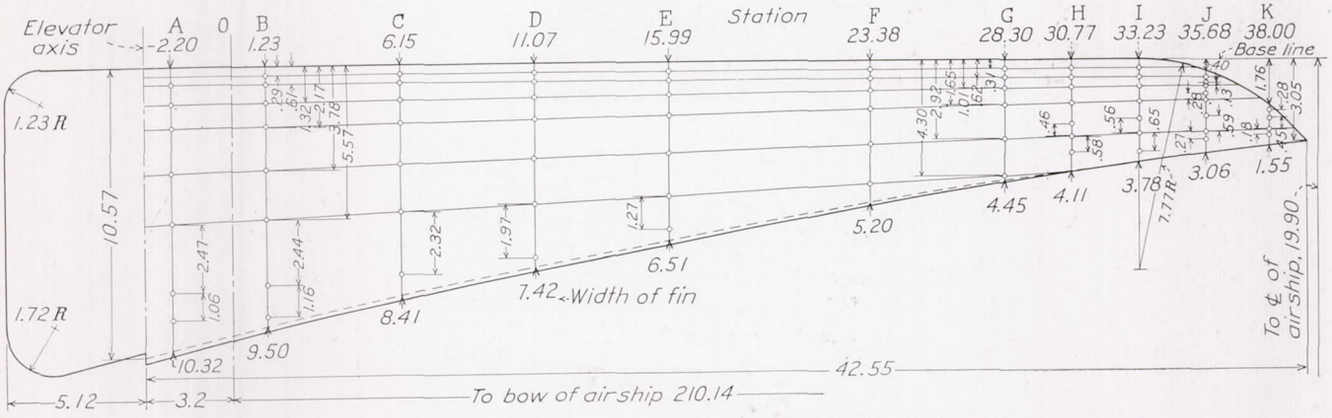

FIGURE 6.—Dimensions and orifice locations. Fin 4; 1/40-scale model of the *Akron;* all dimensions given in inches.

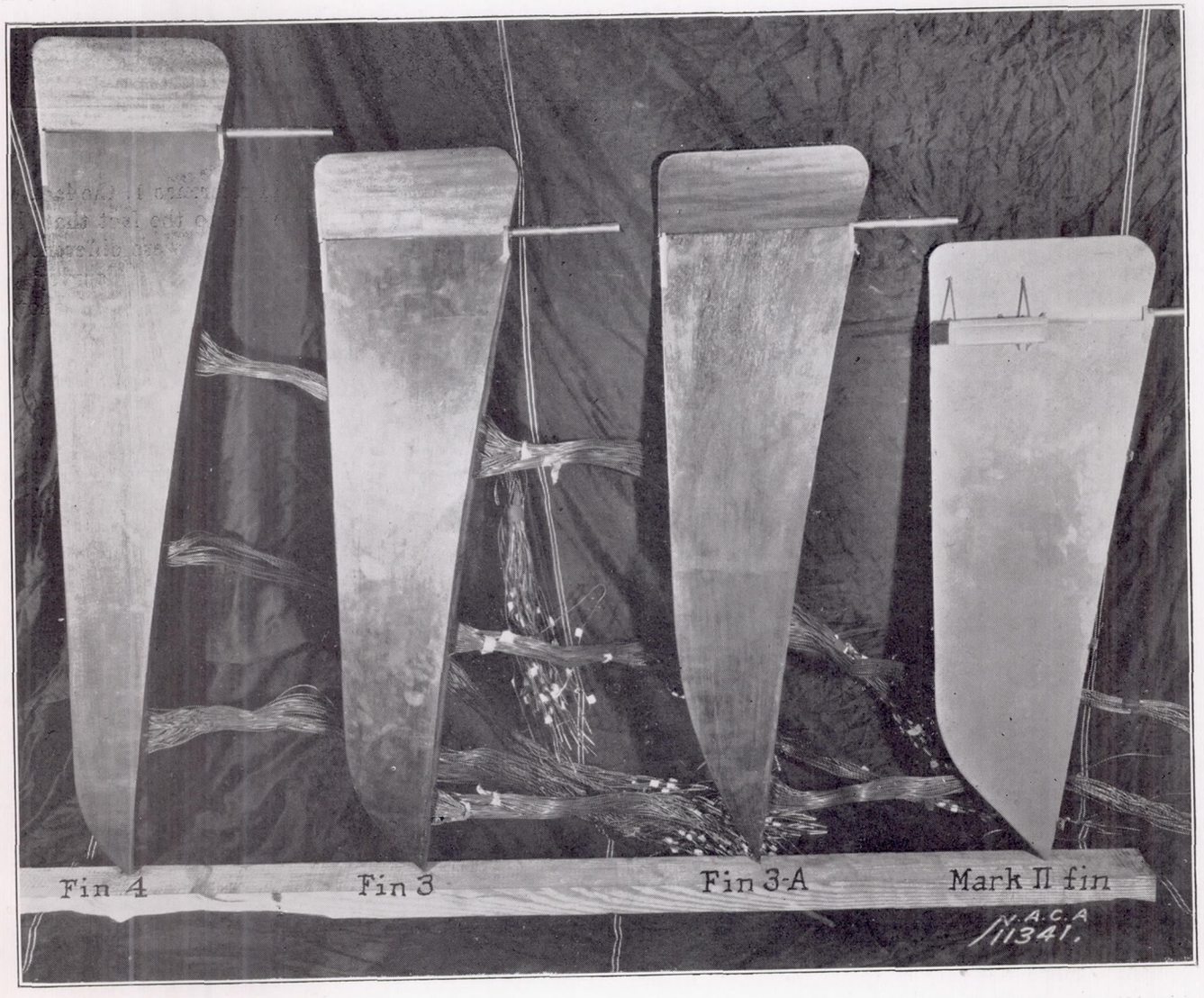

FIGURE 7.—The fins on which pressure-distribution measurements were made.

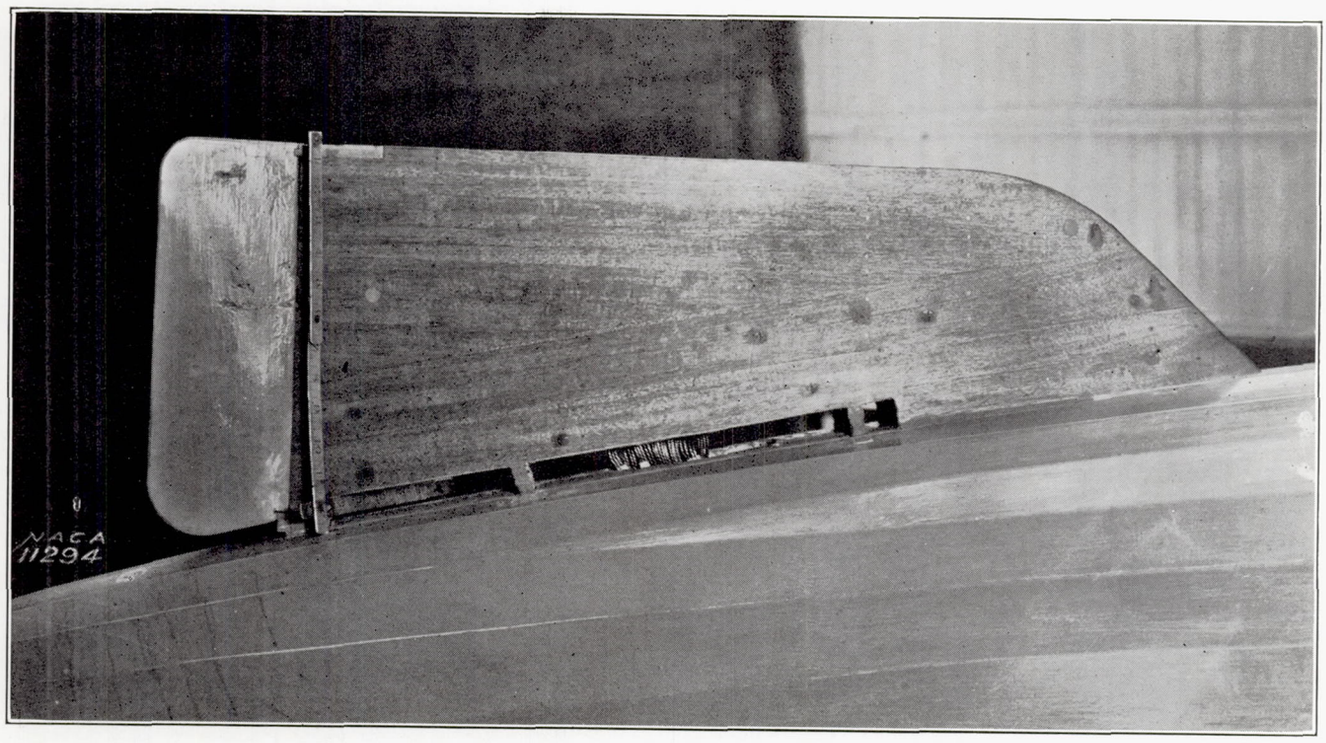

FIGURE 8.—Mark II fin with ¾-inch slot, mounted for tests.

3–A) and the effect of the static-pressure correction would be to shift the position of the pressure diagram without causing any change in the included area. The influence of the static-pressure correction on the point pressures would have been small. A static-pressure survey of the tunnel, made in the absence of the model, showed that the maximum difference between the static pressure in the test chamber and the static

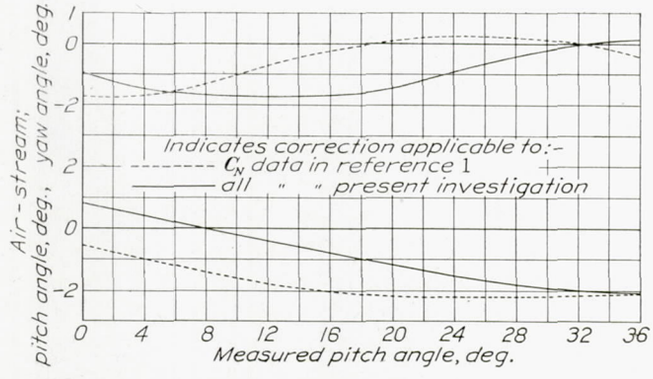

FIGURE 9.—Variation of air-stream angle in region of starboard fin with measured pitch of model.

pressure in the region of the air stream through which pressure measurements were made was of the order of 0.005 q.

A preliminary comparison of the results of these tests with those reported in reference 1 showed poor agreement. Since the only essential difference in the set-ups was the location of the model above the center line of the air stream, 3½ feet for the present tests and 1 foot for the tests reported in reference 1, the lack of agreement was thought to be due to the fact that the flow characteristics of the air stream were different at the two model locations. A stream-angle survey of the air stream confirmed this belief. Figure 9 shows the variation with pitch of the model of the stream angles at the tail of the model. The results have been corrected to take account of the pitch angle in the air stream. No correction has been made to take account of the yaw angle in the air stream.

It is desired to call attention at this time to the fact that the pressures on the upper surfaces of the fins were much greater than had been anticipated. Consequently, at high pitch angles, for the first of the tests made, some of the negative pressures near the tip of the fin were so great that the liquid in the manometer tubes rose above the height of the photostat paper on which the magnitude of the pressures was to be recorded, and consequently no determination could be made of the maximum pressures. In cases where only a few pressures were indeterminate, judgment was used in fairing in the pressure diagrams. In cases where several pressures were indeterminate, the tests in question were repeated at a lower air speed. Eventually all efforts to obtain tests at a high air speed were abandoned and, during the latter part of the program, tests were made at an air speed low enough to insure that all pressures obtained would be recorded on the photostat paper.

In certain cases at high pitch angles where check readings were taken at intervals of approximately 1

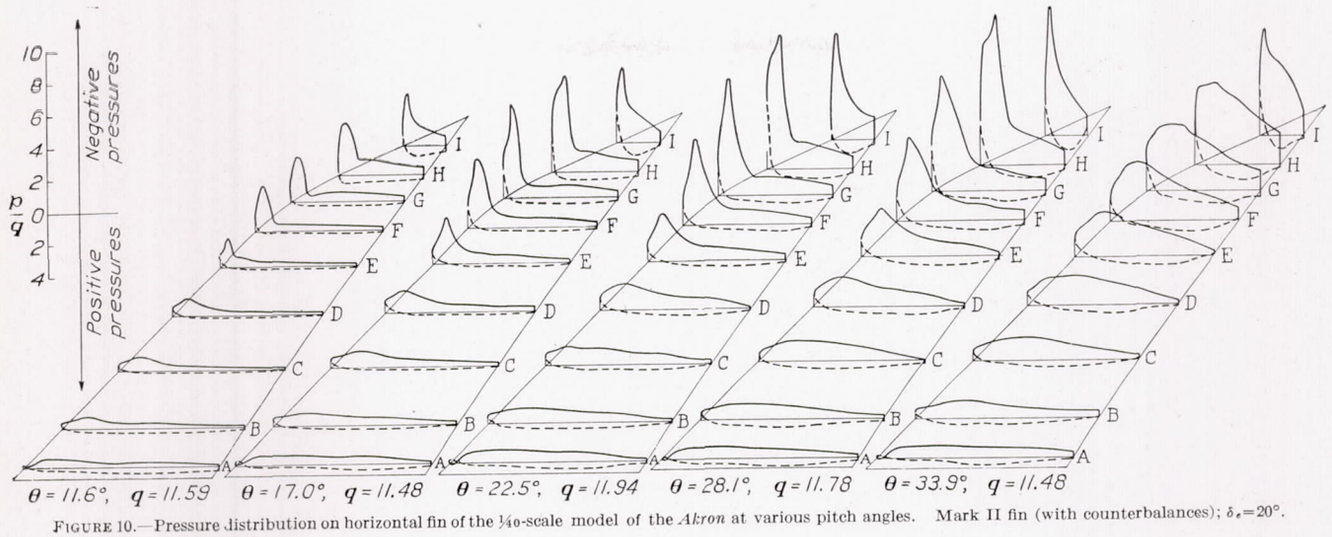

FIGURE 10.—Pressure distribution on horizontal fin of the 1/40-scale model of the *Akron* at various pitch angles. Mark II fin (with counterbalances); $\delta_e = 20°$.

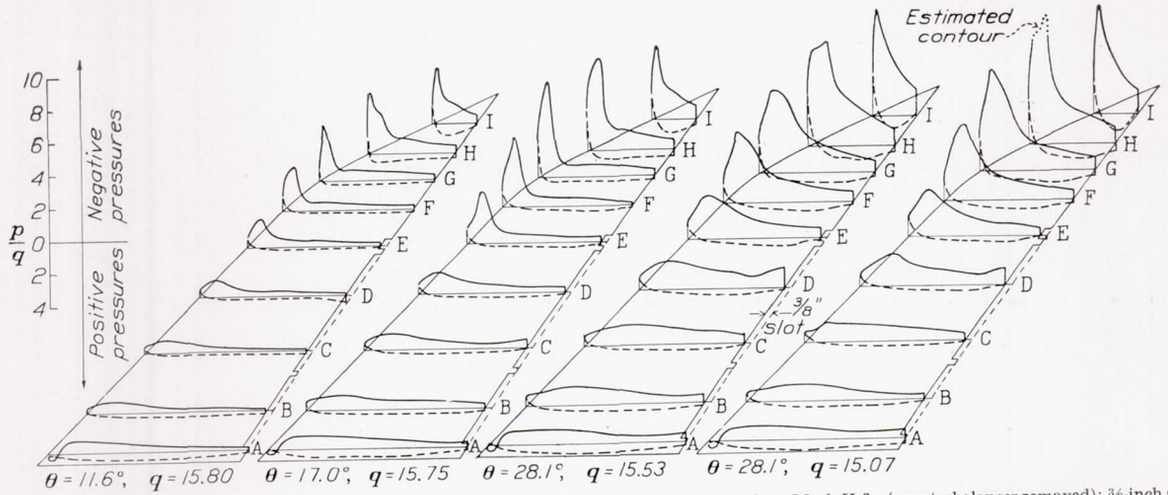

FIGURE 11.—Pressure distribution on horizontal fin of the 1/40-scale model of the *Akron* at various pitch angles. Mark II fin (counterbalances removed); 3/8-inch slot; $\delta_e = 20°$.

minute, a great difference in pressures was recorded. This difference indicated that at extremely high pitch angles (θ=22° to 34°) the forces on the model were fluctuating rapidly, probably owing to instability of the air flow. At times the model was observed to undergo violent spasmodic quivers. This motion was probably due in part to the fluctuation of aerodynamic forces on the tail of the model

Definitions of the terms used in this report follow:

θ, pitch angle.

δ_e, elevator angle.

ω, hull orifice location, measured from keel in degrees.

C_N, $\dfrac{\text{normal force on fins}}{qS}$

q, dynamic pressure ($1/2\ \rho V^2$).

ρ, mass density of the air.

V, air speed.

S, area of fin.

Fin span-chord ratio, $\dfrac{(\text{maximum span of fin})^2}{\text{area of fin}}$

p, observed point pressure.

PRESSURE-DISTRIBUTION MEASUREMENTS ON THE FINS

The magnitude of the maximum pressures and the manner in which the pressure varies over all the fins are illustrated in figures 10 to 15. Large-scale pressure plots of p/q against fin width were made and the pressure diagrams thus formed were graphically integrated to determine the normal force per unit length at each station along the fin. Similarly, the spanwise location of the center of pressure at each longitudinal station on the fin was determined. The values of the normal force per unit length of fin and the moment of that force about the fin root are given in tables II to VII for each station on the fin at which pressure-distribution measurements were made. In order to show the variation of normal force on the fin, there are included, for the various fins tested, typical plots of normal force per unit length against length of fin for the condition of δ_e=20° (figs. 16 to 22). Also included, for the same fins and elevator positions, are charts showing the variation along the fin chord of the moment of the forces on the fin about the fin root (figs. 23 to 27).

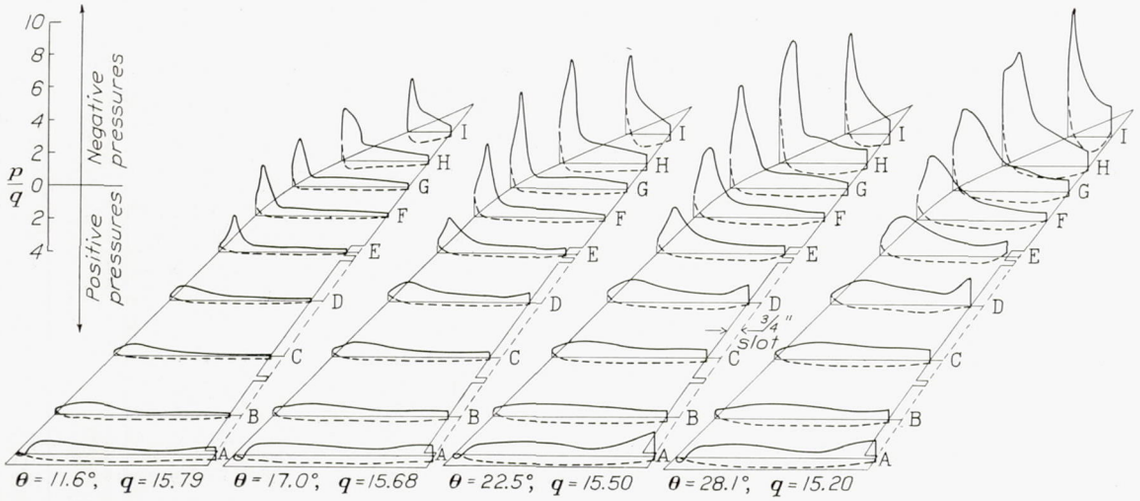

FIGURE 12.—Pressure distribution on horizontal fin of the 1/40-scale model of the *Akron* at various pitch angles. Mark II fin (counterbalances removed); ¾-inch slot; $\delta_e = 20°$.

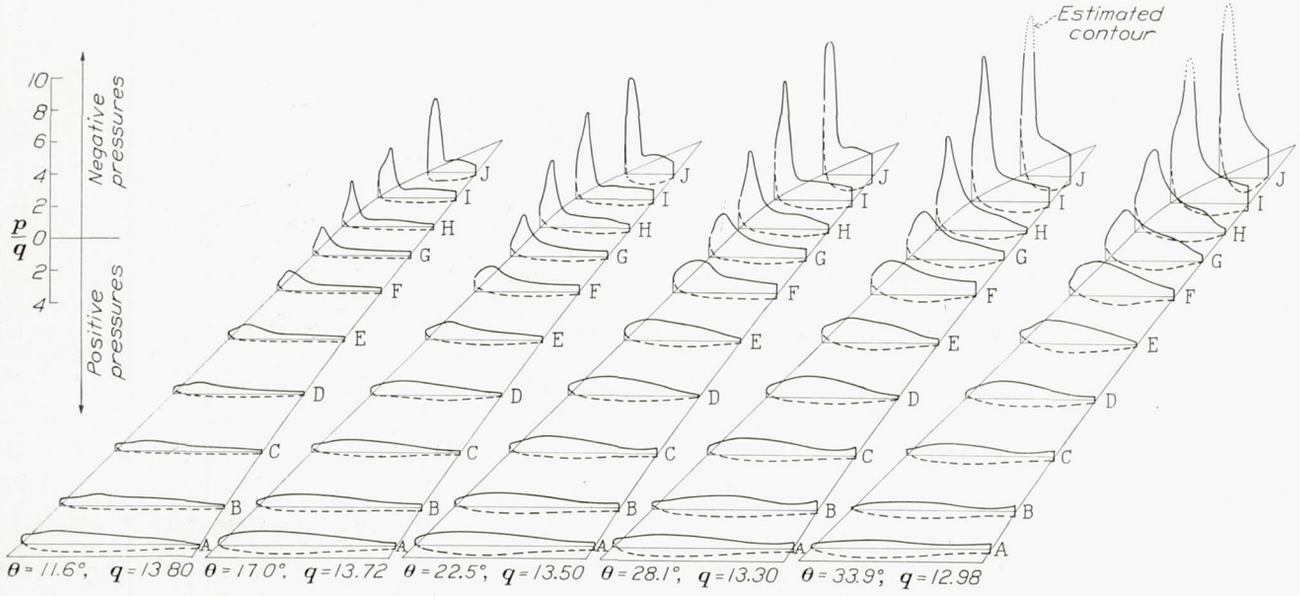

FIGURE 13.—Pressure distribution on horizontal fin of the 1/40-scale model of the *Akron* at various pitch angles. Fin 3; $\delta_e = 20°$.

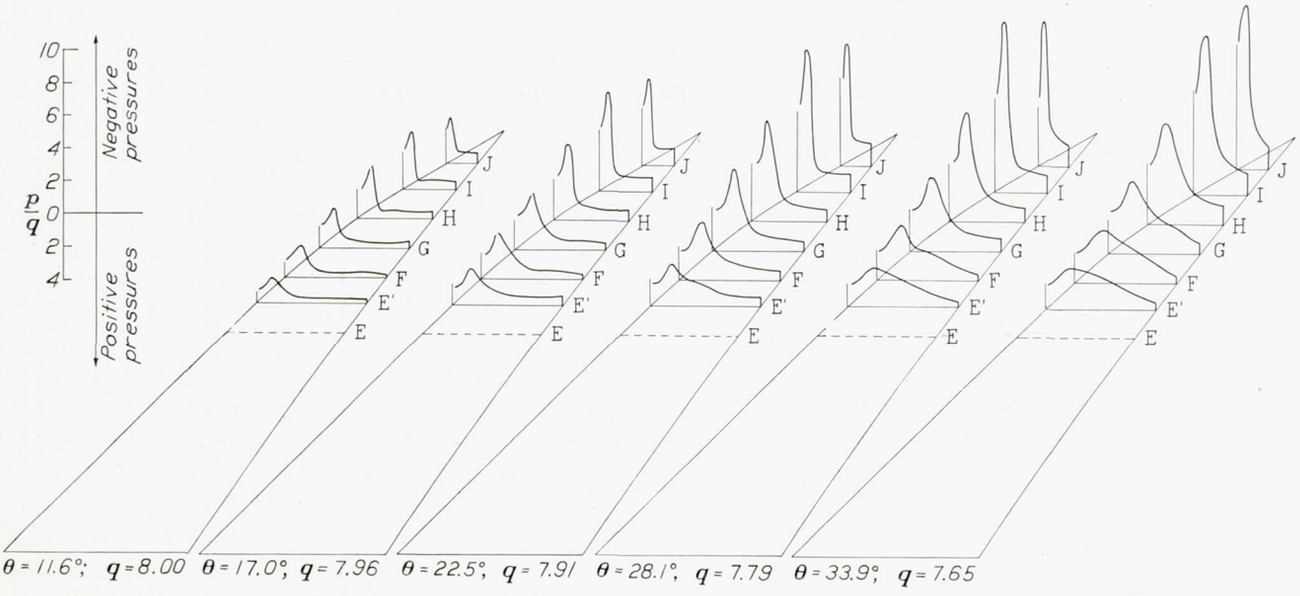

FIGURE 14.—Pressure distribution on upper surface of horizontal fin of the 1/40-scale model of the *Akron* at various pitch angles. Fin 3-A; $\delta_e = 20°$.

Curves showing the variation of normal-force coefficient with pitch angle for various elevator settings are given for the three types of fin tested in figures 28, 29, and 30. Figure 28 also compares the results of these tests of the Mark II fin with those reported in reference 1.

The chordwise location of the center of pressure on the fin was determined from the plots of normal force per unit length against fin length. Values of (normal force)/q and the location of the center of pressure of fin forces are presented in table VIII.

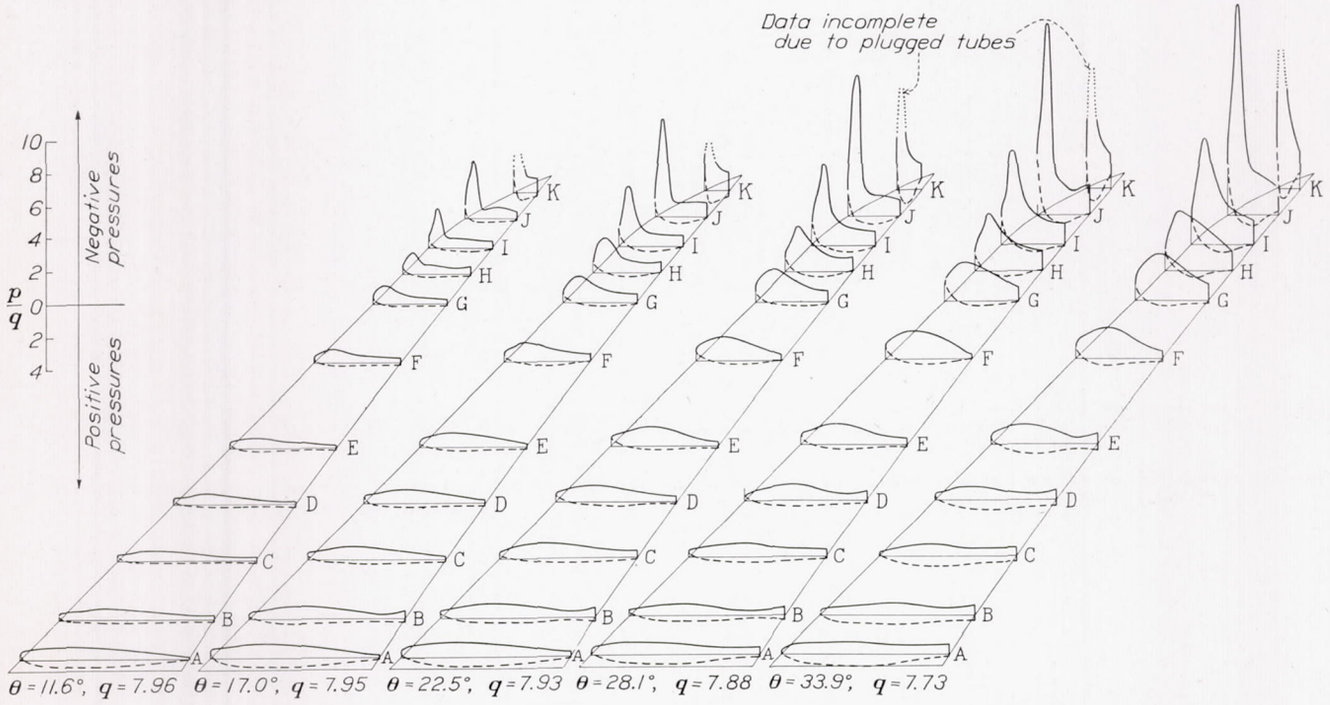

FIGURE 15.—Pressure distribution on horizontal fin of the 1/40-scale model of the *Akron* at various pitch angles. Fin 4; $\delta_e = 20°$.

Figures 31, 32, and 33 show the variation with pitch angle of the maximum point pressure at each station at which pressure-distribution measurements were made.

PRESSURE-DISTRIBUTION MEASUREMENTS ON THE HULL

The value of the transverse force per unit length at any station on the hull is given by the expression

$$f = \frac{dF}{dx} = \int_0^{2\pi} pr \cos \omega d\omega$$

where F is the total transverse force per unit length.

x, the distance from the nose of the hull measured along the longitudinal axis.

r, the radius of the hull.

p, the pressure on the section at a point whose angular distance from the keel is ω.

A graphical solution of this equation was obtained by plotting the pressure at each point on the hull against the projected distance of that point on the horizontal radius of the section. The area of the pressure diagram thus formed gave the transverse force per unit length at the particular station in question.

The integrated values of f from station 14 aft were plotted against distance from the bow of the model. The effect at six angles of pitch of different fins on the transverse force on the hull is shown in figures 34, 35, and 36. There are tabulated in table IX: (1) the total transverse force over the rear portion of the hull, which was obtained from graphical integration of the areas under the curves shown in figures 34, 35, and 36; (2) the moment about the center of buoyancy of the transverse forces on the rear portion of the hull; (3) the normal force on the various fins that were used on the model when the hull pressures were measured; (4) the moment of the fin force about the center of buoyancy; and (5) the total moment of the combined hull and fin forces about the center of buoyancy.

Figure 37 shows the effects of the different fins on the moment, about the center of buoyancy, of the transverse aerodynamic forces acting on the fins and on the rear portion of the hull.

In order to facilitate the application of model test results to a full-scale airship, there is included in table X the location of the structural frames on the *Akron* and their corresponding location on the 1/40-scale model.

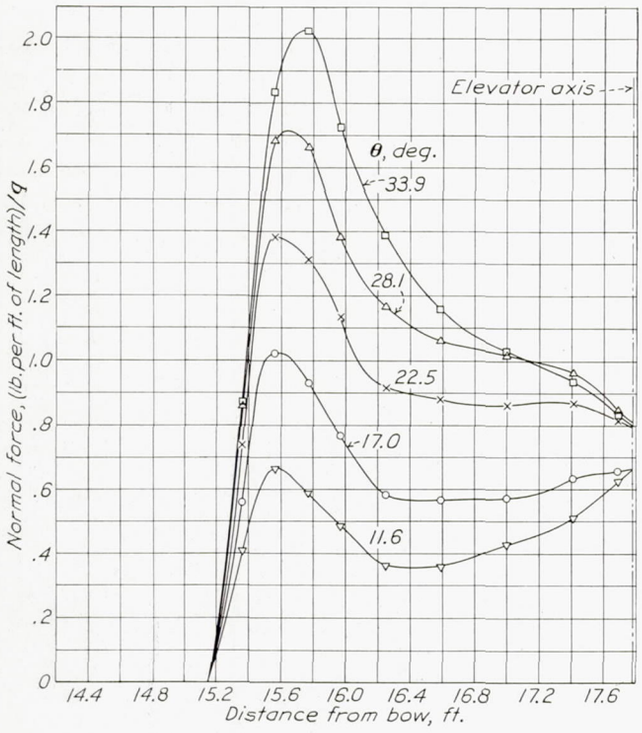

FIGURE 16.—Normal force per unit length on fin of the 1/40-scale model of the *Akron*. Mark II fin (with counterbalances); $\delta_e = 20°$.

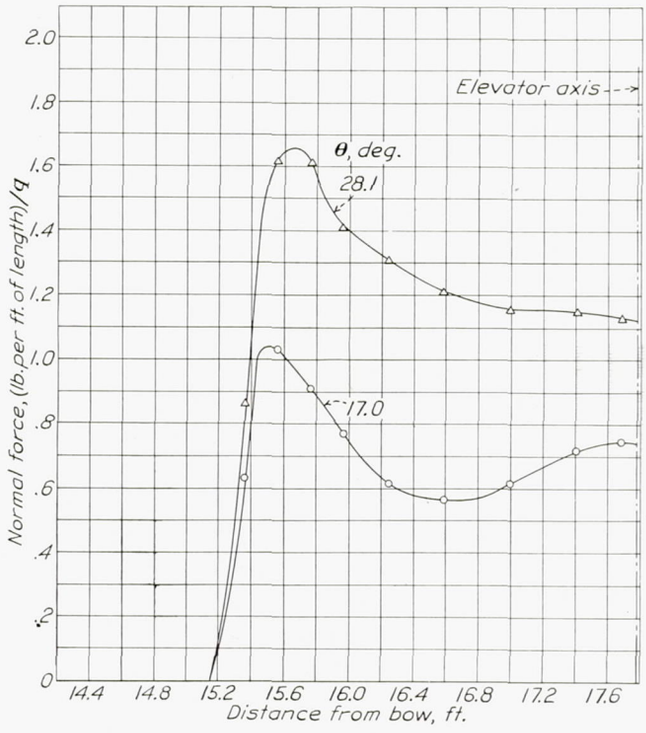

FIGURE 17.—Normal force per unit length on fin of the 1/40-scale model of the *Akron*. Mark II fin (counterbalances removed); $\delta_e = 20°$.

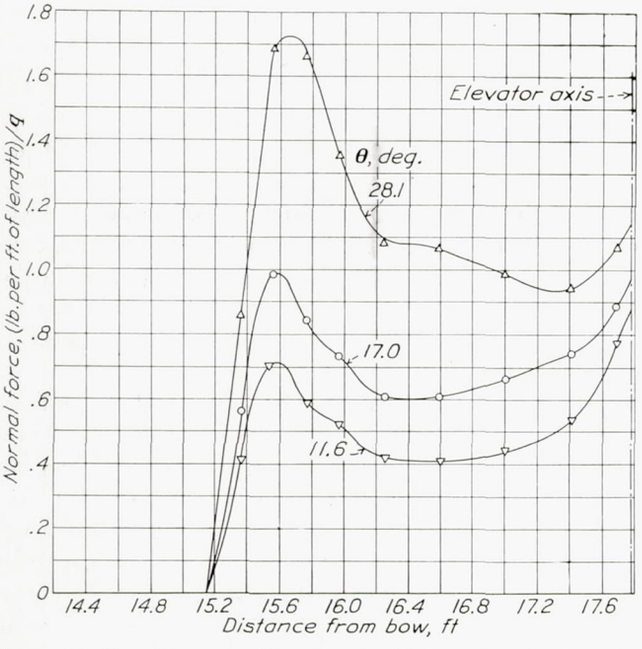

FIGURE 18.—Normal force per unit length on fin of the 1/40-scale model of the *Akron*. Mark II fin (counterbalances removed); 3/8-inch slot; $\delta_e = 20°$.

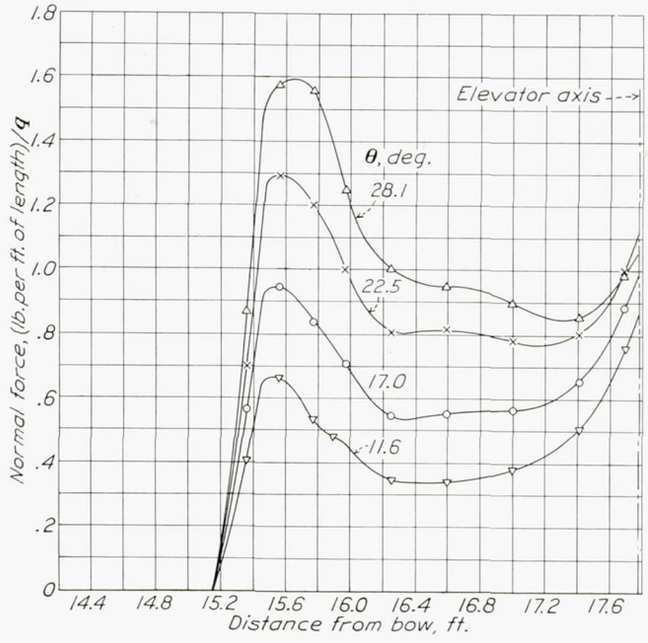

FIGURE 19.—Normal force per unit length on fin of the 1/40-scale model of the *Akron*. Mark II fin (counterbalances removed); 3/4-inch slot; $\delta_e = 20°$.

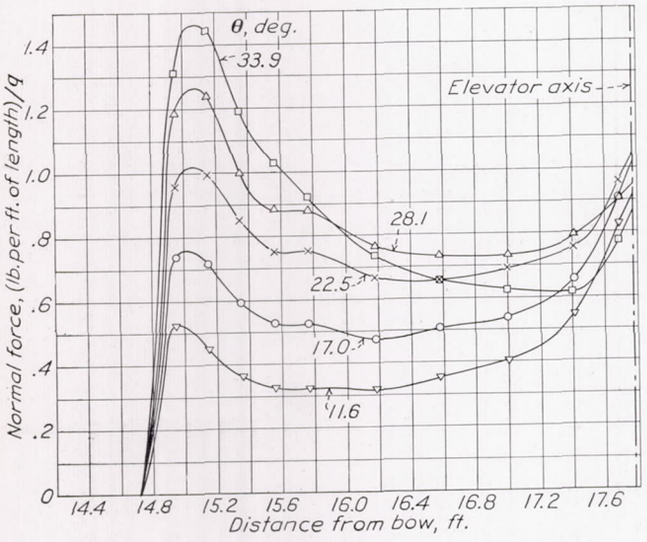

FIGURE 20.—Normal force per unit length on fin of the 1/40-scale model of the *Akron*. Fin 3; $\delta_e=20°$.

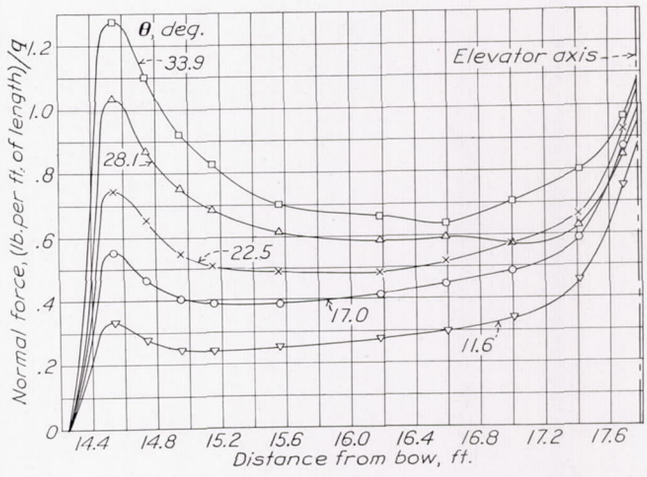

FIGURE 21.—Normal force per unit length on fin of the 1/40-scale model of the *Akron*. Fin 4; $\delta_e=20°$.

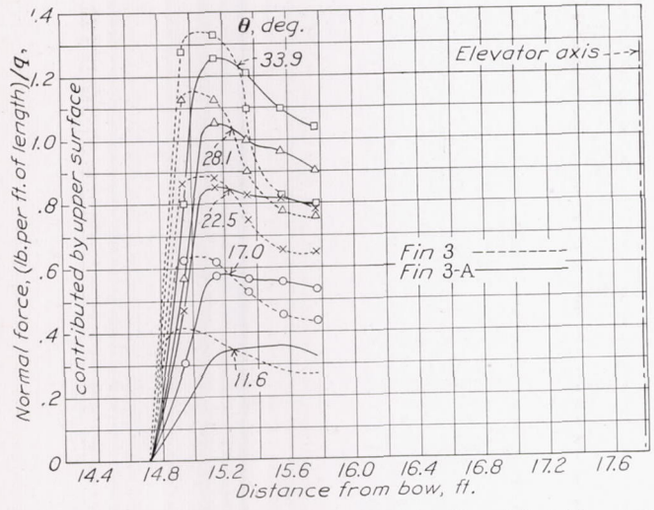

FIGURE 22.—Comparison of normal force per unit length contributed by upper surfaces of fin 3 and fin 3-A of the 1/40-scale model of the *Akron*; $\delta_e=20°$. NOTE.—Pressures on lower surface not measured. Reference pressure is static pressure in test chamber.

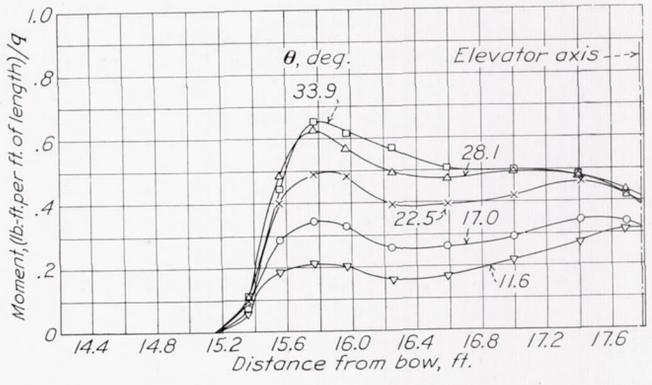

FIGURE 23.—Moment of forces on fin about fin root of the 1/40-scale model of the *Akron*. Mark II fin (with counterbalances); $\delta_e=20°$.

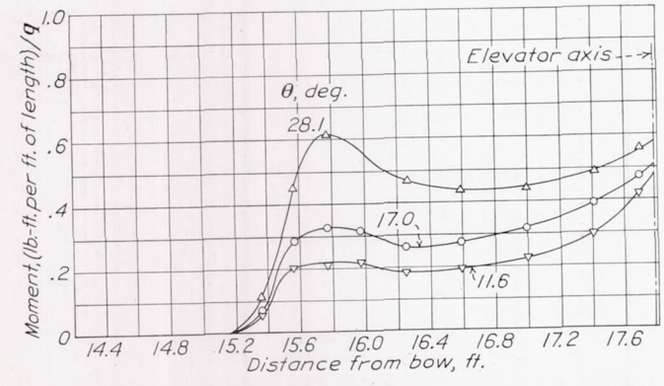

FIGURE 24.—Moment of forces on fin about fin root of the 1/40-scale model of the *Akron*. Mark II fin (counterbalances removed); 3/8-inch slot; $\delta_e=20°$.

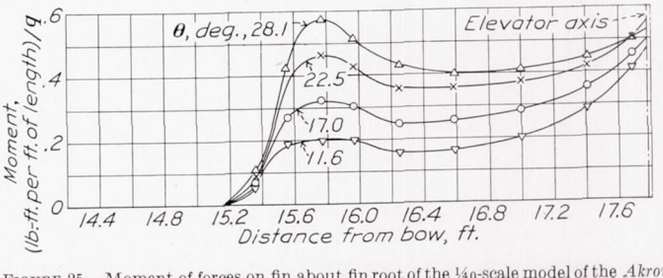

FIGURE 25.—Moment of forces on fin about fin root of the 1/40-scale model of the *Akron*. Mark II fin (counterbalances removed); 3/4-inch slot; $\delta_e=20°$.

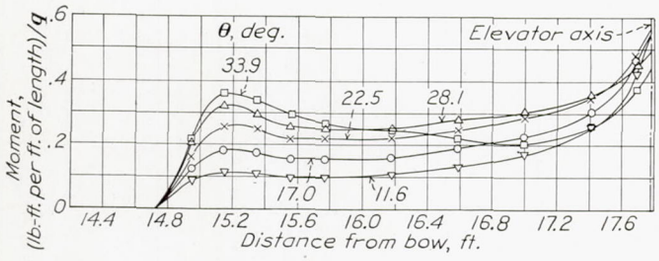

FIGURE 26.—Moment of forces on fin about fin root of the 1/40-scale model of the *Akron*. Fin 3; $\delta_e = 20°$.

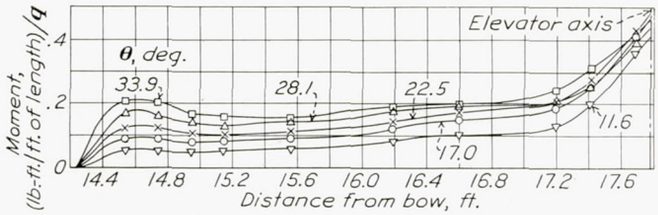

FIGURE 27.—Moment of forces on fin about fin root of the 1/40-scale model of the *Akron*. Fin 4; $\delta_e = 20°$.

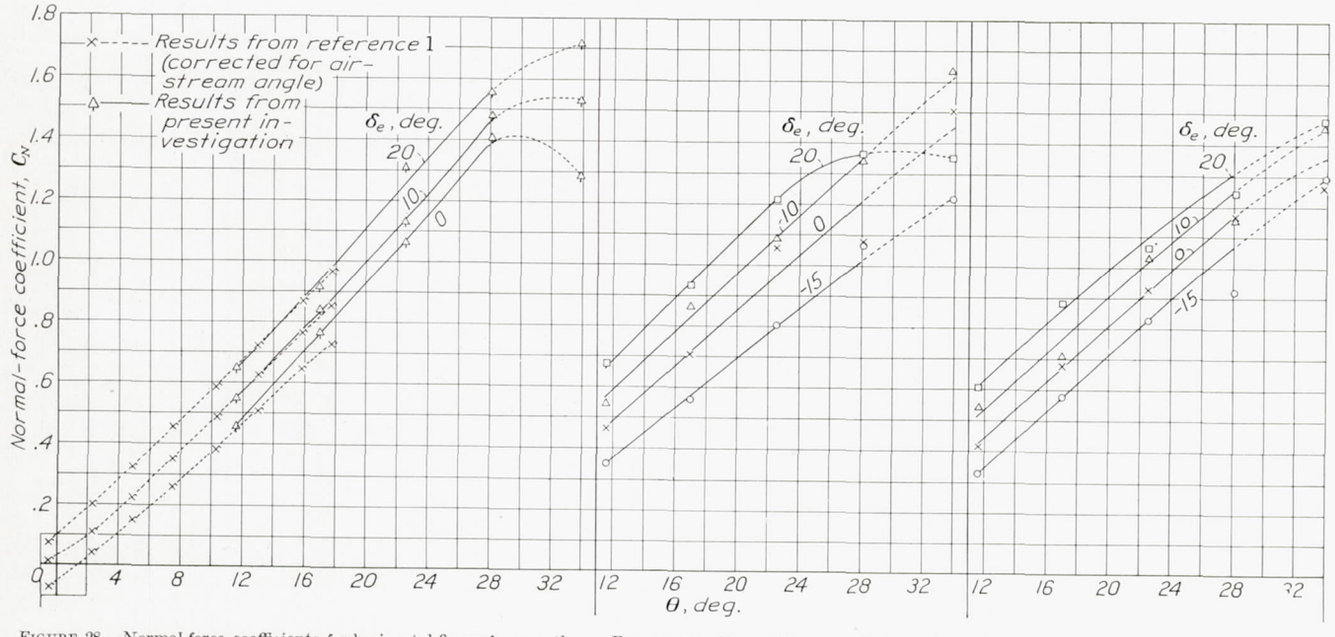

FIGURE 28.—Normal-force coefficients for horizontal fin surfaces on the 1/40-scale model of the *Akron*. Mark II fin (with counterbalances).

FIGURE 29.—Normal-force coefficients for horizontal fin surfaces on the 1/40-scale model of the *Akron*. Fin 3.

FIGURE 30.—Normal-force coefficients for horizontal fin surfaces on the 1/40-scale model of the *Akron*. Fin 4.

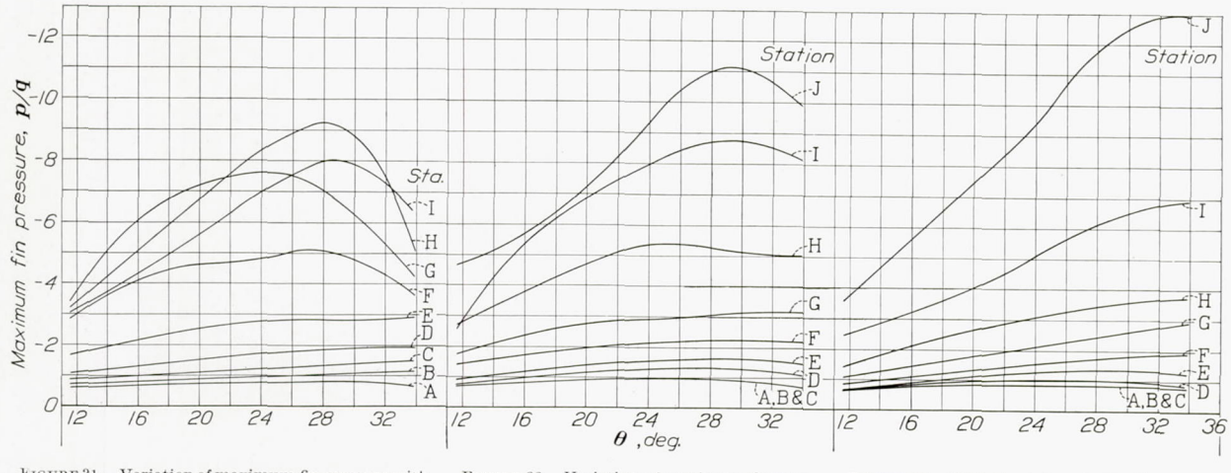

FIGURE 31.—Variation of maximum fin pressure with pitch angle. The 1/40-scale model of the *Akron*; Mark II fin (with counterbalances); $\delta_e = 20°$.

FIGURE 32.—Variation of maximum fin pressure with pitch angle. The 1/40-scale model of the *Akron*; Fin 3; $\delta_e = 20°$.

FIGURE 33.—Variation of maximum fin pressure with pitch angle. The 1/40-scale model of the *Akron*; Fin 4; $\delta_e = 20°$.

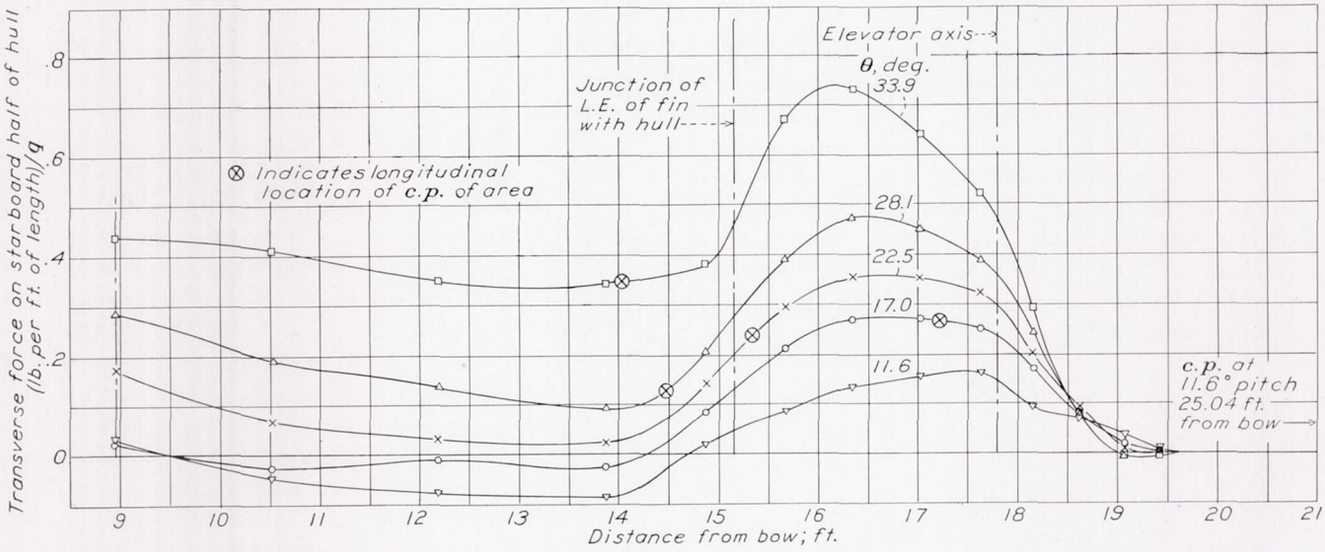

FIGURE 34.—Transverse force per unit length on the hull of the 1/40-scale model of the *Akron*. Mark II fin (counterbalances removed); $\delta_e = 20°$.

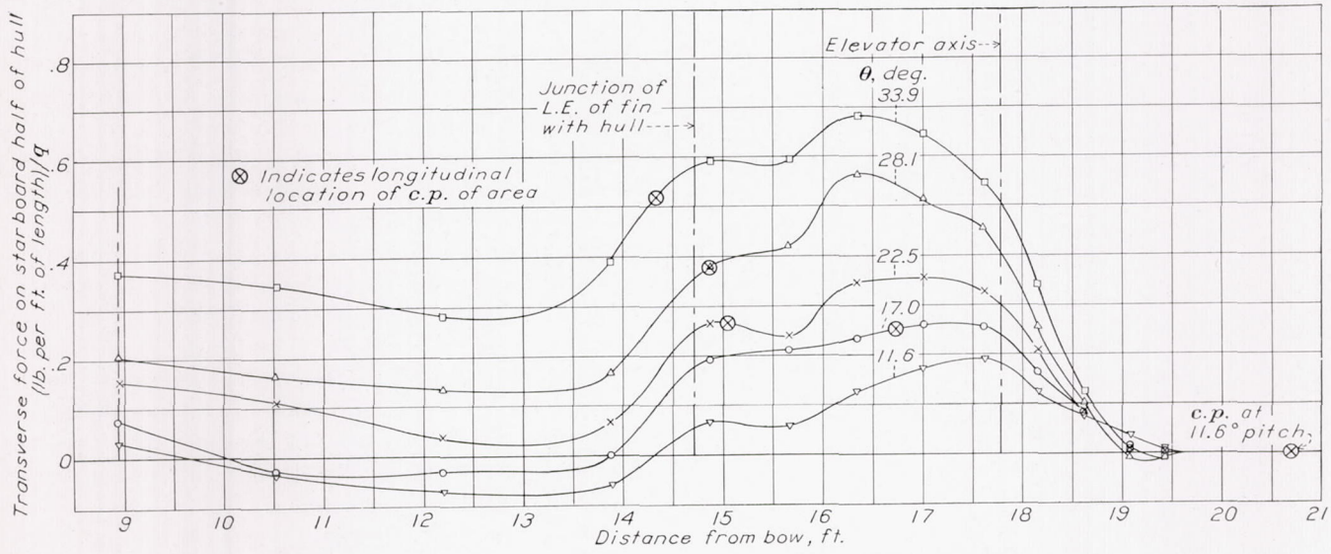

FIGURE 35.—Transverse force per unit length on the hull of the 1/40-scale model of the *Akron*. Fin 3; $\delta_e = 20°$.

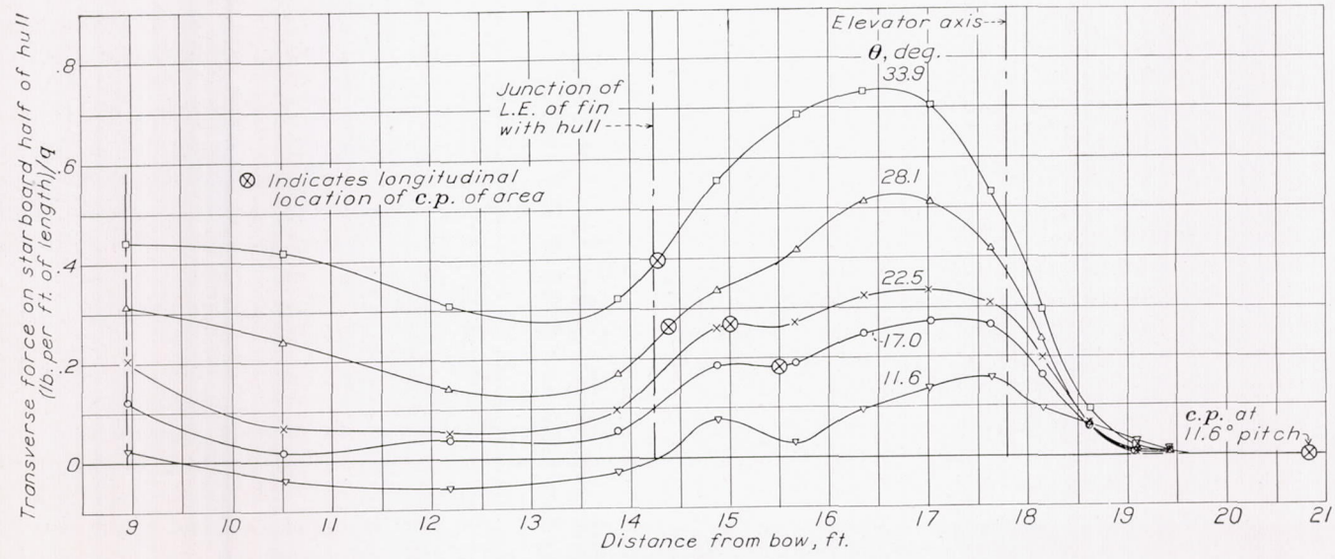

FIGURE 36.—Transverse force per unit length on the hull of the 1/40-scale model of the *Akron*. Fin 4; $\delta_e = 20°$.

DISCUSSION

The results of these tests confirm the conclusions of reference 1 concerning the presence of very large pressures near the leading edge of airship fins. Figures 31, 32, and 33 show that the maximum pressure recorded ($p/q = -13.0$) was obtained at the tip section of fin 4, at the 34° pitch angle. At the same pitch angle the maximum value of p/q obtained on fin 3 was −9.9, and the maximum for the Mark II fin was −6.4. Inspection of figures 31, 32, and 33 also reveals that, although the maximum values of p/q continued to increase on fin 4

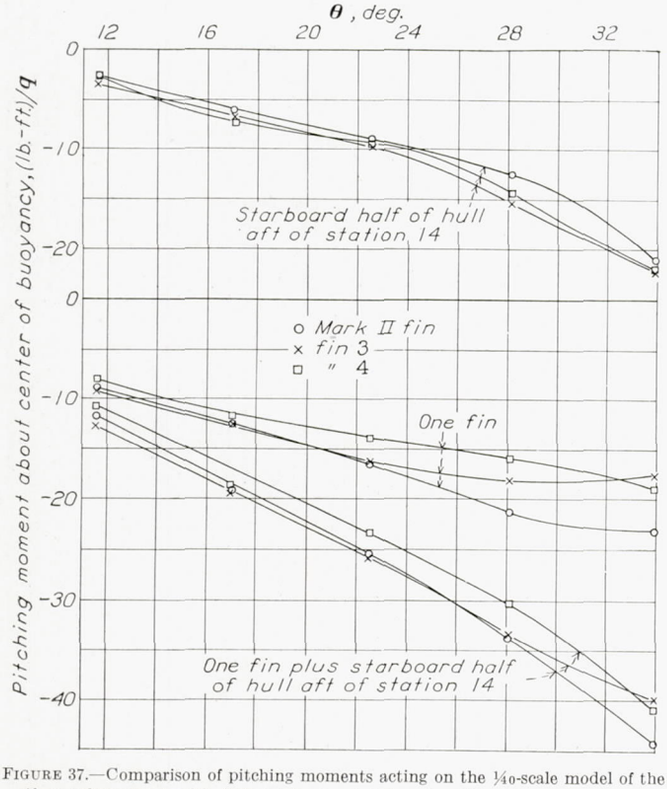

FIGURE 37.—Comparison of pitching moments acting on the 1/40-scale model of the *Akron* when fitted with different horizontal fins; $\delta_e = 20°$. (Forces on elevators neglected.)

up to the maximum angle at which tests were run, the values of p/q obtained on fin 3 reached their maximum value of −11.1 at $\theta = 29°$ and on the Mark II fin the maximum value (−9.2) occurred at $\theta = 28°$. It is of further interest to note that, although at the highest angles of pitch at which tests were made the greatest pressure recorded was that obtained on fin 4, the maximum pressures obtained for all pitch angles below 20° were approximately the same for all fins.

Attention is called to the fact that the pressures cited were obtained from faired curves and that, since the peak pressure would not necessarily occur directly at the points at which the orifices were located and since the slope of the pressure diagram changes from a very large positive value to a very large negative value in the vicinity of the maximum pressure, it is conceivable that greater pressures occurred than those given.

The effect of slots between the hull and fins on the location of the spanwise center of pressure was determined from large-scale pressure diagrams of the type shown in figures 10, 11, and 12. It was observed that neither the ⅜-inch slot nor the ¾-inch slot had much effect at pitch angles below 17°. At higher pitch angles the effect of either slot was to increase the negative pressure at the fin root, thus shifting the center of pressure inboard. The shift was small, however, and was greater for the ⅜-inch slot than for the ¾-inch slot. The maximum movement of center of pressure observed occurred on station D and at $\theta = 30°$ where the movement amounted to about 4 percent of the span of the fin at that station. A comparison of figures 18 and 19 with figure 17 in conjunction with table VIII reveals that at the 17° pitch angle, except for an increase in normal force in the vicinity of the elevator axis, neither slot had an appreciable effect on the normal force or its chordwise distribution on the fin. At higher angles of pitch large fluctuations in forces occurred and the precision of the test results is not considered good enough to draw definite conclusions concerning the effect of the slots. The effect, however, is considered to be small.

Figures 16 to 22 show that fins of low span-chord ratio have a more nearly uniform load distribution along their chord than does the Mark II type of fin, and therefore from structural considerations, provided the effectiveness as shown later is equal, the low span-chord ratio is preferable.

The variation with span-chord ratio of the fin normal-force coefficients can be determined from an inspection of figures 28, 29, and 30. The coefficients for the Mark II fin are, in general, greater than for either of the other fins. At high angles of pitch the coefficients for the Mark II fin begin to decrease with further increase in angle of pitch. The shapes of the curves for the other two fins are not so clearly defined because of erratic results at large angles of pitch.

It is interesting to note from inspection of figures 28, 29, and 30 that the slope of the curves of C_N against θ decreases as the span-chord ratio of the fins decreases. This decrease is in accordance with the principle that the decrease in span-chord ratio decreases the effective aspect ratio of the tail.

It has previously been pointed out in this report that original comparison of these test results did not check the results of reference 2 and that the discrepancy disappeared to a large extent when corrections were made to take account of the air-stream-angle variation in the wind tunnel. Figure 28, which shows values of C_N obtained in these tests and corresponding values of C_N from reference 1 plotted against corrected pitch angle (fig. 9), compares the two sets of data. It is to be noted that agreement is, in general, satisfactory.

The data obtained in these tests indicate that the plan form of the forward part of the fin is an important item in fin design. Figure 22 shows a comparison of the forces acting on the upper surfaces of the tips of fins 3 and 3–A. Pressures were not measured on the lower surface of fin 3–A and it is therefore impossible

to compare the total forces on the two fins. It is believed, however, that a comparison of the forces registered on the upper surfaces shows the relative merits of the two different plan forms. Inspection of figure 22 leads to the conclusion that the effect of modifying the fin tip was to decrease the forces over the forward portion of the fin, presumably because of the decreased fin area forward, and to increase the forces in the region between the elevator axis and the fin tip, thus in effect shifting the center of pressure toward the elevator axis. The peaks of the pressure diagrams occur farther inboard on fin 3–A (fig. 14) than they do on fin 3 (fig. 13); also, the magnitude of the pressures near the fin root is greater on fin 3–A.

A comparison of the chordwise force distribution curves shown in figure 16 with similar curves in figure 17 leads to the conclusion that for the condition of $\delta_e=20°$ the effect of the elevator counterbalances is to decrease the normal force on the rear part of the fin.

The chief criterion in the selection of tail surfaces for airships is the ability of the surfaces to give adequate stability and control. In view of the fact that a large proportion of the stabilizing force obtained with fins is due to the influence of the fins on pressural forces on the hull, it is at once evident that the measurements of forces acting on the fins alone do not give sufficient information for the selection of the most efficient fin. The magnitude of the pressural forces from station 14 aft on the port half of the hull when fitted with the Mark II fin and with fins 3 and 4 is shown in figures 34, 35, and 36, respectively.

The moment about the center of buoyancy of the forces represented by the area under the curves shown in figures 34, 35, and 36 is shown as a function of angle of pitch in figure 37. It is believed that, since pressure-distribution measurements were made on all of that portion of the hull over which the fins appear appreciably to influence the hull forces, the curves of pitching moment against angle of pitch (fig. 37) present a valid comparison of the relative stability characteristics of the airship when fitted with the various fins tested. Attention is called to the fact that, since the pressure-distribution measurements from which this chart is derived were made at but one elevator deflection ($\delta_e=20°$), a complete analysis is impossible. It is believed, however, that the same relative effects as here shown would obtain for other elevator deflections.

Inspection of figure 37 indicates that at extremely high pitch angles ($\theta=34°$) the pitching moment about the center of buoyancy due to pressural forces on the rear half of the hull is approximately equal to the corresponding moment due to the forces on the fins themselves. From the curves in the lower part of figure 37 it is to be seen that, except at angles of pitch greater than 26°, the stabilizing moment obtained when the airship is fitted with the Mark II fin is very nearly equal to the stabilizing moment obtained with fin 3. At angles of pitch greater than 26° the Mark II fin is somewhat superior. With the exception of a slight superiority over fin 3 at extremely high pitch angles, fin 4 is inferior to both of the other fins.

It is desired to point out that, although the narrow fins appear to compare quite favorably with the Mark II fins, the results here shown are not conclusive in that they do not show the effect of the various fins on drag. It is possible that, if the drag of the different fins could be compared on the basis of either equal lift or equal moment coefficients, the fins of low span-chord ratio would show up to disadvantage.

CONCLUSIONS

1. At angles of pitch below about 20° the maximum pressure measured was approximately the same for all fins, regardless of span-chord ratio.

2. At angles of pitch above 20° the maximum fin pressures increase with decreasing span-chord ratio, the highest pressure recorded ($p/q=-13.0$) being that obtained on fin 4 at a pitch angle of 34°.

3. Slots between the hull and fins, of the type here tested, had but little effect on either maximum fin pressures or the position of the center of pressure of fin forces.

4. The plan form of the forward portion of the fin is a critical factor influencing the pressure distribution on the fin.

5. The pitching moment about the center of buoyancy contributed by the rear half of the hull increases with pitch until at an angle of 33° it is approximately equal to the moment contributed by the fins.

6. At any given angle of pitch up to 26° the restoring moment of the model when fitted with the Mark II fin was slightly less than that obtained with fin 3 and appreciably greater than that obtained with fin 4.

7. Neglecting the effect on drag, it appears that fin 3, owing to its relatively low bending moment about the fin root, has certain structural advantages over the Mark II fin.

Langley Memorial Aeronautical Laboratory,
National Advisory Committee for Aeronautics,
Langley Field, Va., *April 4, 1937.*

REFERENCES

1. Freeman, Hugh B.: Pressure-Distribution Measurements on the Hull and Fins of a 1/40-Scale Model of the U. S. Airship *Akron*. T. R. No. 443, N. A. C. A., 1932.
2. Freeman, Hugh B.: Force Measurements on a 1/40-Scale Model of the U. S. Airship *Akron*. T. R. No. 432, N. A. C. A., 1932.
3. Weick, Fred E., and Wood, Donald H.: The Twenty-Foot Propeller Research Tunnel of the National Advisory Committee for Aeronautics. T. R. No. 300, N. A. C. A., 1928.

TABLE I

DIMENSIONS OF THE 1/40-SCALE MODEL "AKRON"

[Length, 19.62 ft.; volume, 115.00 cu. ft.; location of elevator axis, $(x/L)=0.9059$; center of buoyance, $(x/L)=0.464$.]

Distance from bow / length $\frac{x}{L}$	Radius (circumscribed circle) (in.)	Distance from bow / length $\frac{x}{L}$	Radius (circumscribed circle) (in.)
0.00	0.00	0.50	19.80
.02	4.95	.55	19.59
.05	9.96	.60	19.12
.10	14.20	.65	18.46
.15	16.65	.70	17.50
.20	18.39	.75	16.15
.25	19.12	.80	14.44
.30	19.61	.85	12.29
.35	19.85	.90	9.61
.40	19.90	.95	6.52
.45	19.90	1.00	.00

Fin	Area of one fin (without elevator) (sq. ft.)	Area of elevator (sq. ft.)	Area of elevator counterbalance (sq. ft.)	Elevator chord (ft.)	Maximum chord of fin (ft.)	Maximum span of fin (ft.)	Fin span-chord ratio $\frac{(\text{maximum span of fin})^2}{(\text{area of fin})}$
Mark II	1.850	0.356	0.110	0.396	2.63	1.028	0.570
3	1.858	.356	.....	.402	3.06	.943	.479
3-A	1.775	.356	.....	.402	3.06	.943	.500
4	1.838	.356	.....	.427	3.55	.880	.421

TABLE II

NORMAL FORCE PER UNIT LENGTH OF FIN AND MOMENT OF NORMAL FORCE ABOUT FIN ROOT OF 1/40–SCALE MODEL "AKRON"

MARK II FIN (WITH COUNTERBALANCES)

Station	Distance from bow (ft.)	δ_e (deg.)	Normal force (lb. per ft. length) /q					Moment (ft.-lb. per ft. length) /q				
			θ (deg.)					θ (deg.)				
			11.6	17.0	22.5	28.1	33.9	11.6	17.0	22.5	28.1	33.9
Elevator axis	17.78	0	0.160	0.241	0.295	0.336	0.286	0.106	0.160	0.179	0.204	0.170
A	17.69		.195	.302	.361	.424	.325	.120	.185	.214	.253	.185
B	17.41		.253	.425	.527	.666	.412	.146	.242	.296	.380	.233
C	17.00		.254	.470	.635	.855	.545	.140	.246	.325	.430	.293
D	16.59		.276	.492	.716	1.005	.745	.110	.230	.324	.448	.358
E	16.25		.341	.565	.815	1.135	1.105	.157	.250	.351	.484	.475
F	15.97		.415	.715	1.013	1.391	1.546	.176	.305	.430	.565	.593
G	15.77		.502	.850	1.255	1.673	1.835	.184	.320	.480	.623	.625
H	15.56		.610	.945	1.312	1.665	1.755	.170	.266	.375	.467	.440
I	15.36		.361	.531	.710	.885	.980	.050	.067	.095	.118	.122
Tip of fin	15.15		.000	.000	.000	.000	.000	.000	.000	.000	.000	.000
Elevator axis	17.78	10	0.429	0.486	0.522	0.590	0.573	0.231	0.260	0.280	0.310	0.286
A	17.69		.420	.496	.553	.655	.603	.230	.268	.305	.353	.313
B	17.41		.383	.515	.635	.808	.694	.217	.284	.354	.447	.375
C	17.00		.345	.536	.710	.944	.827	.181	.274	.356	.463	.417
D	16.59		.322	.543	.755	1.033	.985	.153	.255	.340	.459	.442
E	16.25		.364	.574	.823	1.155	1.225	.161	.255	.360	.566	.515
F	15.97		.431	.740	1.046	1.380	1.614	.183	.308	.445	.565	.620
G	15.77		.515	.844	1.224	1.645	1.975	.192	.320	.470	.622	.670
H	15.56		.632	.973	1.335	1.655	1.885	.178	.276	.385	.475	.465
I	15.36		.366	.535	.702	.866	1.005	.146	.070	.092	.118	.125
Tip of fin	15.15		.000	.000	.000	.000	.000	.000	.000	.000	.000	.000
Elevator axis	17.78	20	0.660	0.665	0.794	0.810	0.800	0.312	0.320	0.395	0.412	0.388
A	17.69		.623	.656	.815	.845	.833	.312	.335	.415	.435	.420
B	17.41		.512	.634	.867	.965	.935	.276	.340	.460	.477	.480
C	17.00		.427	.571	.860	1.015	1.028	.220	.290	.418	.491	.500
D	16.59		.362	.567	.880	1.060	1.158	.171	.261	.391	.474	.507
E	16.25		.363	.581	.916	1.165	1.390	.160	.260	.395	.493	.565
F	15.97		.485	.763	1.133	1.380	1.725	.201	.325	.481	.568	.620
G	15.77		.585	.930	1.315	1.665	2.025	.210	.340	.486	.622	.648
H	15.56		.661	1.019	1.383	1.680	1.833	.185	.285	.400	.482	.445
I	15.36		.406	.557	.735	.855	.870	.052	.073	.095	.110	.110
Tip of fin	15.15		.000	.000	.000	.000	.000	.000	.000	.000	.000	.000

TABLE III

NORMAL FORCE PER UNIT LENGTH OF FIN ON 1/40-SCALE MODEL "AKRON"

MARK II FIN (COUNTERBALANCES REMOVED)

Station	Distance from bow (ft.)	δ_e (deg.)	Normal force (lb. per ft. length)/q				
			θ (deg.)				
			11.6	17.0	22.5	28.1	33.9
Elevator axis	17.78	20		0.740		1.122	
A	17.69			.744		1.130	
B	17.41			.713		1.147	
C	17.00			.612		1.156	
D	16.59			.564		1.213	
E	16.25			.615		1.306	
F	15.97			.768		1.415	
G	15.77			.908		1.612	
H	15.56			1.030		1.620	
I	15.36			.620		.860	
Tip of fin	15.15			.000		.000	

TABLE IV

NORMAL FORCE PER UNIT LENGTH OF FIN AND MOMENT OF NORMAL FORCE ABOUT FIN ROOT OF 1/40-SCALE MODEL "AKRON"

MARK II FIN, 3/8-INCH SLOT (COUNTERBALANCES REMOVED)

Station	Distance from bow (ft.)	δ_e (deg.)	Normal force (lb. per ft. length)/q					Moment (lb.-ft. per ft. length)/q				
			θ (deg.)					θ (deg.)				
			11.6	17.0	22.5	28.1	33.9	11.6	17.0	22.5	28.1	33.9
Elevator axis	17.78	20	0.875	0.971		1.143		0.475	0.508		0.575	
A	17.69		.774	.888		1.075		.418	.474		.560	
B	17.41		.535	.743		.945		.295	.393		.490	
C	17.00		.437	.664		.990		.224	.318		.442	
D	16.59		.410	.608		1.065		.193	.276		.435	
E	16.25		.420	.608		1.090		.184	.263		.462	
F	15.97		.520	.732		1.360		.216	.314		.565	
G	15.77		.590	.843		1.660		.219	.323		.610	
H	15.56		.712	.988		1.700		.202	.283		.450	
I	15.36		.413	.562		.860		.055	.071		.113	
Tip of fin	15.15		.000	.000		.000		.000	.000		.000	

TABLE V

NORMAL FORCE PER UNIT LENGTH OF FIN AND MOMENT OF NORMAL FORCE ABOUT FIN ROOT OF 1/40-SCALE MODEL "AKRON"

MARK II FIN, 3/4-INCH SLOT (COUNTERBALANCES REMOVED)

Station	Distance from bow (ft.)	δ_e (deg.)	Normal force (lb. per ft. length)/q					Moment (lb.-ft. per ft. length)/q				
			θ (deg.)					θ (deg.)				
			11.6	17.0	22.5	28.1	33.9	11.6	17.0	22.5	28.1	33.9
Elevator axis	17.78	20	0.875	0.986	1.116	1.055		0.467	0.495	0.555	0.525	
A	17.69		.754	.885	1.002	.985		.413	.450	.506	.500	
B	17.41		.505	.658	.808	.855		.288	.354	.421	.445	
C	17.00		.380	.565	.782	.900		.200	.285	.370	.410	
D	16.59		.339	.550	.810	.950		.164	.253	.358	.402	
E	16.25		.345	.545	.810	1.005		.160	.250	.360	.430	
F	15.97		.459	.706	1.002	1.250		.196	.304	.428	.515	
G	15.77		.530	.841	1.203	1.560		.200	.320	.460	.575	
H	15.56		.661	.944	1.293	1.575		.183	.268	.370	.425	
I	15.36		.404	.565	.700	.870		.053	.070	.088	.110	
Tip of fin	15.15		.000	.000	.000	.000		.000	.000	.000	.000	

TABLE VI

NORMAL FORCE PER UNIT LENGTH OF FIN AND MOMENT OF NORMAL FORCE ABOUT FIN ROOT OF 1/40-SCALE MODEL "AKRON"

FIN 3

Station	Distance from bow (ft.)	δ_e (deg.)	Normal force (lb. per ft. length)/q					Moment (lb.-ft. per ft. length)/q				
			θ (deg.)					θ (deg.)				
			11.6	17.0	22.5	28.1	33.9	11.6	17.0	22.5	28.1	33.9
Elevator axis	17.78	−15	−0.280	−0.300	−0.233	−0.147	−0.008	−0.115	−0.089	−0.057	−0.020	0.011
A	17.69		−.140	−.160	−.077	.022	.100	−.036	−.016	.002	.036	.068
B	17.41		.108	.142	.234	.304	.365	.066	.092	.128	.157	.170
C	17.00		.173	.285	.396	.493	.494	.084	.133	.180	.218	.208
D	16.59		.221	.345	.476	.603	.565	.090	.133	.187	.230	.222
E	16.18		.224	.365	.526	.685	.696	.080	.130	.179	.228	.240
F	15.77		.260	.425	.626	.825	.936	.081	.135	.181	.243	.278
G	15.56		.278	.478	.665	.926	1.115	.088	.145	.196	.266	.312
H	15.35		.335	.558	.755	1.066	1.296	.100	.166	.224	.304	.363
I	15.15		.435	.675	.715	1.265	1.563	.110	.175	.238	.322	.370
J	14.95		.450	.700	.943	1.195	1.372	.075	.117	.166	.204	.220
Tip of fin	14.72		.000	.000	.000	.000	.000	.000	.000	.000	.000	.000
Elevator axis	17.78	0	0.176	0.245	0.322	0.270	0.378	0.106	0.158	0.198	0.160	0.210
A	17.69		.200	.275	.383	.303	.443	.116	.160	.210	.161	.225
B	17.41		.264	.335	.494	.373	.591	.130	.165	.235	.180	.262
C	17.00		.263	.370	.565	.475	.719	.120	.163	.246	.203	.290
D	16.59		.243	.392	.610	.546	.804	.094	.150	.233	.210	.296
E	16.18		.266	.390	.633	.593	.910	.084	.134	.208	.200	.292
F	15.77		.288	.443	.715	.776	1.065	.089	.133	.203	.221	.304
G	15.56		.298	.482	.736	.875	1.160	.093	.143	.216	.256	.324
H	15.35		.351	.570	.814	1.008	1.305	.104	.168	.242	.300	.363
I	15.15		.455	.743	1.026	1.256	1.504	.113	.190	.263	.318	.360
J	14.95		.468	.736	1.045	1.247	1.545	.086	.120	.175	.208	.240
Tip of fin	14.72		.000	.000	.000	.000	.000	.000	.000	.000	.000	.000
Elevator axis	17.78	10	0.514	0.665	0.690	0.700	0.738	0.290	0.353	0.373	0.374	0.390
A	17.69		.473	.605	.656	.677	.735	.254	.323	.345	.348	.365
B	17.41		.375	.506	.585	.663	.765	.182	.244	.280	.304	.336
C	17.00		.316	.484	.582	.708	.863	.137	.206	.250	.300	.343
D	16.59		.294	.473	.592	.742	.906	.114	.180	.228	.280	.337
E	16.18		.276	.464	.627	.774	.983	.100	.157	.210	.257	.313
F	15.77		.287	.504	.675	.867	1.127	.090	.155	.200	.254	.321
G	15.56		.288	.540	.706	.930	1.125	.090	.164	.206	.265	.336
H	15.35		.347	.624	.805	1.063	1.275	.106	.183	.235	.307	.358
I	15.15		.446	.746	.975	1.263	1.504	.113	.190	.256	.325	.368
J	14.95		.480	.755	1.020	1.203	1.500	.074	.125	.175	.205	.245
Tip of fin	14.72		.000	.000	.000	.000	.000	.000	.000	.000	.000	.000
Elevator axis	17.78	20	0.916	1.020	1.043	0.947	0.867	0.542	0.550	0.568	0.494	0.445
A	17.69		.822	.910	.955	.905	.775	.428	.467	.486	.452	.375
B	17.41		.543	.656	.756	.792	.615	.255	.304	.347	.356	.260
C	17.00		.404	.538	.688	.732	.626	.170	.226	.288	.302	.205
D	16.59		.352	.504	.655	.730	.655	.135	.190	.246	.280	.220
E	16.18		.318	.473	.667	.765	.735	.110	.160	.220	.253	.245
F	15.77		.323	.522	.753	.874	.918	.100	.108	.220	.250	.268
G	15.56		.326	.525	.756	.880	1.030	.100	.108	.218	.257	.296
H	15.35		.362	.592	.850	.994	1.192	.110	.126	.250	.295	.338
I	15.15		.445	.715	.995	1.235	1.443	.111	.134	.255	.320	.355
J	14.95		.525	.737	.955	1.185	1.313	.088	.126	.161	.204	.215
Tip of fin	14.72		.000	.000	.000	.000	.000	.000	.000	.000	.000	.000

TABLE VII

NORMAL FORCE PER UNIT LENGTH OF FIN AND MOMENT OF NORMAL FORCE ABOUT FIN ROOT OF 1/40-SCALE MODEL "AKRON"

FIN 4

Station	Distance from bow (ft.)	δ_e (deg.)	Normal force (lb. per ft. length)/q					Moment (lb.-ft. per ft. length)/q				
			θ (deg.)					θ (deg.)				
			11.6	17.0	22.5	28.1	33.9	11.6	17.0	22.5	28.1	33.9
Elevator axis	17.78	−15	−0.195	−0.167	−0.062	−0.100	0.000	−0.073	−0.047	0.000	−0.010	0.025
A	17.69		−.119	−.056	.030	.014	.161	−.038	.000	.040	.025	.093
B	17.41		.057	.190	.280	.240	.534	.039	.095	.130	.108	.225
C	17.00		.148	.295	.405	.290	.745	.065	.122	.156	.120	.265
D	16.59		.213	.330	.430	.422	.785	.073	.110	.148	.142	.244
E	16.18		.214	.335	.444	.495	.705	.067	.098	.134	.150	.195
F	15.56		.214	.336	.468	.559	.675	.051	.080	.110	.135	.157
G	15.15		.210	.340	.516	.655	.720	.047	.070	.104	.130	.140
H	14.95		.227	.357	.565	.740	.748	.044	.074	.108	.140	.140
I	14.74		.262	.415	.654	.870	.875	.048	.083	.125	.164	.164
J	14.54		.305	.512	.755	.992	1.035	.049	.084	.120	.160	.174
K	14.35		.135	.203	.275	.333	.385	.020	.031	.041	.075	.100
Tip of fin	14.23		.000	.000	.000	.000	.000	.000	.000	.000	.000	.000
Elevator axis	17.78	0	0.210	0.305	0.388	0.357	0.370	0.123	0.160	0.203	0.190	0.181
A	17.69		.196	.295	.390	.410	.394	.104	.150	.192	.202	.185
B	17.41		.180	.306	.413	.516	.495	.084	.141	.180	.212	.208
C	17.00		.214	.356	.475	.565	.695	.088	.140	.180	.204	.233
D	16.59		.218	.367	.495	.592	.635	.077	.123	.165	.192	.207
E	16.18		.213	.360	.480	.602	.618	.063	.104	.140	.175	.178
F	15.56		.220	.355	.481	.606	.612	.051	.081	.110	.142	.142
G	15.15		.212	.355	.504	.660	.735	.043	.072	.102	.130	.140
H	14.95		.226	.375	.535	.712	.790	.043	.076	.105	.135	.146
I	14.74		.263	.434	.650	.820	.915	.051	.083	.122	.152	.168
J	14.54		.324	.509	.747	.965	1.084	.050	.085	.125	.161	.184
K	14.35		.160	.205	.248	.370	.508	.017	.036	.053	.092	.114
Tip of fin	14.23		.000	.000	.000	.000	.000	.000	.000	.000	.000	.000
Elevator axis	17.78	10	0.550	0.650	0.738	0.602	0.620	0.255	0.305	0.350	0.268	0.300
A	17.69		.453	.560	.655	.545	.637	.227	.270	.313	.260	.295
B	17.41		.322	.400	.540	.453	.695	.147	.175	.232	.232	.287
C	17.00		.275	.361	.525	.572	.793	.110	.143	.200	.216	.275
D	16.59		.277	.373	.522	.523	.775	.100	.130	.172	.170	.234
E	16.18		.287	.338	.483	.521	.735	.088	.100	.143	.152	.208
F	15.56		.265	.325	.494	.572	.714	.058	.072	.114	.135	.165
G	15.15		.240	.344	.533	.670	.742	.050	.072	.108	.130	.145
H	14.95		.245	.374	.558	.736	.735	.050	.075	.108	.133	.145
I	14.74		.274	.418	.667	.870	.924	.052	.079	.125	.162	.170
J	14.54		.326	.492	.744	1.008	1.106	.053	.080	.120	.169	.185
K	14.35		.160	.230	.470	.620	.815	.021	.035	.052	.070	.086
Tip of fin	14.23		.000	.000	.000	.000	.000	.000	.000	.000	.000	.000
Elevator axis	17.78	20	0.878	0.990	1.050	0.950	1.082	0.412	0.470	0.485	0.440	0.467
A	17.69		.746	.874	.922	.845	.963	.355	.410	.430	.392	.425
B	17.41		.453	.588	.662	.625	.800	.197	.253	.276	.256	.310
C	17.00		.338	.487	.575	.575	.705	.130	.185	.206	.205	.245
D	16.59		.296	.450	.514	.590	.635	.103	.150	.170	.190	.200
E	16.18		.272	.415	.484	.584	.660	.085	.122	.145	.176	.190
F	15.56		.249	.389	.485	.613	.700	.060	.090	.112	.145	.158
G	15.15		.240	.390	.505	.684	.825	.052	.084	.102	.133	.162
H	14.95		.244	.407	.546	.750	.925	.048	.081	.108	.140	.168
I	14.74		.278	.464	.652	.867	1.100	.053	.090	.125	.162	.202
J	14.54		.332	.555	.743	1.033	1.275	.054	.090	.125	.172	.205
K	14.35		.125	.170	.213	.260	.365	.018	.037	.055	.071	.118
Tip of fin	14.23		.000	.000	.000	.000	.000	.000	.000	.000	.000	.000

TABLE VIII

VALUES OF $\frac{\text{NORMAL FORCE}}{q}$ AND DISTANCES OF CENTER OF PRESSURE OF FIN FORCES FROM ELEVATOR AXIS FOR VARIOUS FINS TESTED ON 1/40-SCALE MODEL "AKRON"

[Values of $\frac{\text{normal force}}{q}$ are for one fin only]

δ_e (deg.)	θ (deg.)	Normal force (lb.)/q						Distance of center of pressure from elevator axis (ft.)					
		Mark II fin (with counter-balances)	Mark II fin (counter-balances removed)	Mark II fin (⅜-in. slot)	Mark II fin (¾-in. slot)	Fin 3	Fin 4	Mark II fin (with counter-balances)	Mark II fin (counter-balances removed)	Mark II fin (⅜-in. slot)	Mark II fin (¾-in. slot)	Fin 3	Fin 4
−15	11.6	.....	.....	.....	.....	0.65	0.61	.....	.....	.....	.....	1.96	2.15
	17.0	.....	.....	.....	.....	1.05	1.06	.....	.....	.....	.....	1.94	2.01
	22.5	.....	.....	.....	.....	1.50	1.52	.....	.....	.....	.....	1.87	2.01
	28.1	.....	.....	.....	.....	2.00	1.70	.....	.....	.....	.....	1.87	2.17
	33.9	.....	.....	.....	.....	2.27	2.39	.....	.....	.....	.....	1.91	1.88
0	11.6	0.84	.....	.....	.....	.87	.77	1.47	.....	.....	.....	1.64	1.82
	17.0	1.42	.....	.....	.....	1.31	1.25	1.44	.....	.....	.....	1.70	1.81
	22.5	1.96	.....	.....	.....	1.96	1.71	1.47	.....	.....	.....	1.68	1.83
	28.1	2.60	.....	.....	.....	2.01	2.14	1.47	.....	.....	.....	1.83	1.88
	33.9	2.37	.....	.....	.....	2.80	2.32	1.60	.....	.....	.....	1.76	1.91
10	11.6	1.02	.....	.....	.....	1.01	1.00	1.33	.....	.....	.....	1.49	1.63
	17.0	1.56	.....	.....	.....	1.60	1.31	1.38	.....	.....	.....	1.55	1.69
	22.5	2.09	.....	.....	.....	2.03	1.89	1.41	.....	.....	.....	1.60	1.76
	28.1	2.74	.....	.....	.....	2.50	2.12	1.41	.....	.....	.....	1.65	1.92
	33.9	2.85	.....	.....	.....	3.05	2.68	1.48	.....	.....	.....	1.67	1.82
20	11.6	1.20	.....	1.29	1.16	1.25	1.11	1.25	.....	1.23	1.23	1.34	1.45
	17.0	1.70	1.77	1.80	1.68	1.74	1.63	1.34	1.30	1.25	1.28	1.44	1.56
	22.5	2.24	.....	.....	2.27	2.25	1.96	1.34	.....	.....	1.31	1.51	1.64
	28.1	2.88	3.15	2.89	2.67	2.53	2.28	1.36	1.30	1.34	1.36	1.57	1.79
	33.9	3.18	.....	.....	.....	2.52	2.73	1.40	.....	.....	.....	1.70	1.81

TABLE IX

NORMAL FORCE ON FINS AND HULL AND PITCHING MOMENT ABOUT CENTER OF BUOYANCY OF FINS AND AFTER PART OF HULL OF 1/40-SCALE MODEL "AKRON"

[Values are for one fin and starboard half of hull aft of station 14; $\delta_e = 20°$.]

Fin	θ (deg.)	$\frac{\text{Transverse force}}{q}$ on hull $\left(\frac{\text{lb.}}{q}\right)$	$\frac{M_{c.b.}}{q}$ of forces on hull $\left(\frac{\text{ft.-lb.}}{q}\right)$	$\frac{\text{Normal force}}{q}$ on fin $\left(\frac{\text{lb.}}{q}\right)$	$\frac{M_{c.b.}}{q}$ of force on fin $\left(\frac{\text{ft.-lb.}}{q}\right)$	$\frac{\text{Transverse force}}{q}$ on hull plus $\frac{\text{Normal force}}{q}$ on fin $\left(\frac{\text{lb.}}{q}\right)$	$\frac{M_{c.b.}}{q}$ of forces on hull and fin $\left(\frac{\text{ft.-lb.}}{q}\right)$
Mark II (with counterbalances)	11.6	0.17	−2.7	1.20	−8.9	1.37	−11.6
	17.0	.78	−6.3	1.70	−12.5	2.48	−18.8
	22.5	1.44	−9.0	2.24	−16.4	3.68	−25.4
	28.1	2.33	−12.5	2.88	−21.1	5.21	−33.6
	33.9	4.25	−21.0	3.18	−23.1	7.43	−44.1
3	11.6	.30	−3.6	1.25	−9.2	1.55	−12.8
	17.0	.89	−6.8	1.74	−12.6	2.63	−19.4
	22.5	1.65	−9.8	2.25	−16.1	3.90	−25.9
	28.1	2.65	−15.3	2.53	−18.0	5.18	−33.3
	33.9	4.21	−22.1	2.51	−17.5	6.72	−39.6
4	11.6	.23	−2.7	1.11	−8.0	1.34	−10.7
	17.0	1.14	−7.3	1.63	−11.6	2.77	−18.9
	22.5	1.63	−9.6	1.96	−13.8	3.59	−23.4
	28.1	2.73	−14.4	2.28	−15.7	5.01	−30.1
	33.9	4.35	−22.0	2.73	−18.8	7.08	−40.8

TABLE X

LOCATION OF STRUCTURAL FRAMES ON U. S. AIRSHIP "AKRON" AND THEIR CORRESPONDING LOCATION ON A 1/40-SCALE MODEL

Ring location from 0 station (full-scale) (meters)	Ring location from bow (1/40-scale model) (feet)	Ring location from 0 station (full-scale) (meters)	Ring location from bow (1/40-scale model) (feet)
0	17.51	125.0	7.26
17.5	16.08	147.5	5.41
35.0	14.64	170.0	3.57
57.5	12.80	187.5	2.13
80.0	10.95	198.75	1.21
102.5	9.10	210.75	.23

U. S. GOVERNMENT PRINTING OFFICE: 1937

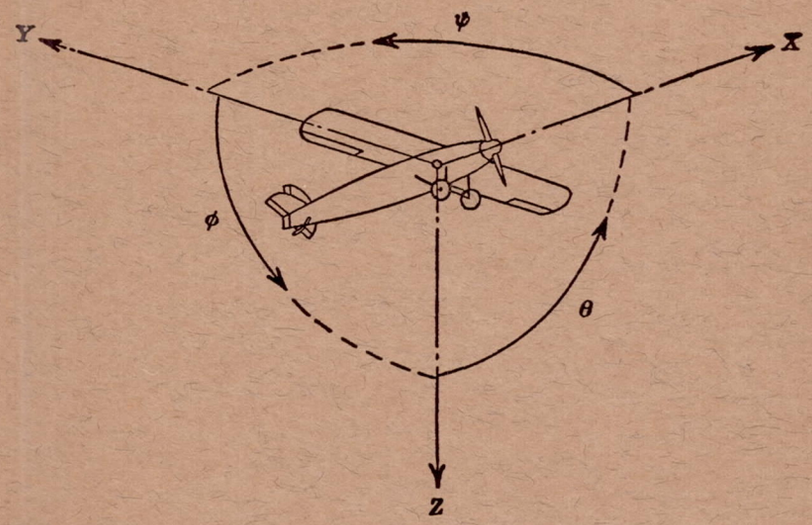

Positive directions of axes and angles (forces and moments) are shown by arrows

Axis		Force (parallel to axis) symbol	Moment about axis			Angle		Velocities	
Designation	Symbol		Designation	Symbol	Positive direction	Designation	Symbol	Linear (component along axis)	Angular
Longitudinal	X	X	Rolling	L	$Y \longrightarrow Z$	Roll	ϕ	u	p
Lateral	Y	Y	Pitching	M	$Z \longrightarrow X$	Pitch	θ	v	q
Normal	Z	Z	Yawing	N	$X \longrightarrow Y$	Yaw	ψ	w	r

Absolute coefficients of moment

$C_l = \frac{L}{qbS}$ (rolling) $\quad C_m = \frac{M}{qcS}$ (pitching) $\quad C_n = \frac{N}{qbS}$ (yawing)

Angle of set of control surface (relative to neutral position), δ. (Indicate surface by proper subscript.)

4. PROPELLER SYMBOLS

D, Diameter

p, Geometric pitch

p/D, Pitch ratio

V', Inflow velocity

V_s, Slipstream velocity

T, Thrust, absolute coefficient $C_T = \frac{T}{\rho n^2 D^4}$

Q, Torque, absolute coefficient $C_Q = \frac{Q}{\rho n^2 D^5}$

P, Power, absolute coefficient $C_P = \frac{P}{\rho n^3 D^5}$

C_s, Speed-power coefficient $= \sqrt[5]{\frac{\rho V^5}{P n^2}}$

η, Efficiency

n, Revolutions per second, r.p.s.

Φ, Effective helix angle $= \tan^{-1}\left(\frac{V}{2\pi r n}\right)$

5. NUMERICAL RELATIONS

1 hp.=76.04 kg-m/s=550 ft-lb./sec.

1 metric horsepower=1.0132 hp.

1 m.p.h.=0.4470 m.p.s.

1 m.p.s.=2.2369 m.p.h.

1 lb.=0.4536 kg.

1 kg=2.2046 lb.

1 mi.=1,609.35 m=5,280 ft.

1 m=3.2808 ft.